Title: The Notch Ligand Jagged1 is Required for the Formation, Maintenance, and Survival of Hensen Cells in the Mouse Cochlea.

Elena Chrysostomou[1, *], Luyi Zhou[2, *], Yuanzhao L. Darcy[2], Kaley A. Graves[2], Angelika Doetzlhofer[1, $], and Brandon C. Cox[2,3, $]

1. The Solomon H. Snyder Department of Neuroscience and Center for Sensory Biology, Johns Hopkins University School of Medicine, Baltimore, Maryland, 21205

2. Departments of Pharmacology and 3. Otolaryngology, Southern Illinois University School of Medicine, Springfield, Illinois, 62702

* Denotes co-first authors, $ denotes co-corresponding authors

Corresponding authors email addresses:

Angelika Doetzlhofer: adoetzlhofer@jhmi.edu

Brandon C. Cox: bcox@siumed.edu

ABSTRACT

During cochlear development, the Notch ligand JAGGED 1 (JAG1) plays an important role in the specification of the prosensory region, which gives rise to sound-sensing hair cells and neighboring supporting cells (SCs). While JAG1's expression is maintained in SCs through adulthood, the function of JAG1 in SC development is unknown. Here, we demonstrate that JAG1 is essential for the formation and maintenance of Hensen cells (HeCs), a highly specialized SC-subtype located at the edge of the auditory epithelium. Deletion of *Jag1* at the onset of differentiation, at stage E14.5, disrupted HeC formation. Similar loss of HeCs was observed when *Jag1* was deleted at P0/P1 and fate-mapping analysis revealed that in the absence of *Jag1* some HeCs die, but others convert into neighboring Claudius cells. In support of a role for JAG1 in cell survival, genes involved in mitochondrial function and protein synthesis were downregulated in P0 cochlea lacking *Jag1*.

INTRODUCTION

The canonical Notch signaling cascade plays multiple roles in the development of sensory structures in the vertebrate inner ear. In this pathway, activation of the Notch receptor by membrane-bound ligands located on neighboring cells leads to the release of the Notch intercellular domain, which as part of a larger transcription complex, activates the transcription downstream target genes (Kopan and Ilagan, 2009).

During inner ear sensory development, Notch signaling operates through two distinct modes of signaling, lateral inhibition and lateral induction (Eddison et al., 2000, Daudet and Zak, 2020). Notch-mediated lateral induction first defines and maintains the

prosensory domains that give rise to highly specialized sensory epithelia composed of hair cells (HCs) and surrounding supporting cells (SCs). The Notch ligand JAGGED1 (JAG1) and the downstream transcription factor SOX2 are essential for the early role of Notch signaling in prosensory progenitor specification and maintenance (Daudet and Lewis, 2005, Hartman et al., 2010, Pan et al., 2010, Neves et al., 2011) and early loss of JAG1 abolishes or greatly reduces the pool of inner ear prosensory progenitors (Brooker et al., 2006, Kiernan et al., 2006, Petrovic et al., 2014).

As prosensory progenitor cells differentiate into HCs and SCs during late embryogenesis, Notch signaling plays a key role in limiting the number of HCs that form in a process termed lateral inhibition. Activated by ATOH1, a transcriptional activator and master regulator of HC formation (Bermingham et al., 1999, Chen et al., 2002, Woods et al., 2004), nascent HCs express the Notch ligands *Delta-like 1* (*Dll1*), *Delta-like 3* (*Dll3*), and *Jagged 2* (*Jag2*) (Adam et al., 1998, Lanford et al., 1999, Morrison et al., 1999, Hartman et al., 2007). Activation of Notch 1 receptor signaling by DLL1 and JAG2 in adjacent prosensory progenitor cells inhibits these cells from becoming HCs (Lanford et al., 1999, Kiernan et al., 2005, Brooker et al., 2006).

Important effectors of this HC-repressive function mediated by Notch signaling are members of the HES/HEY family. HES/HEY proteins are transcriptional repressors, which antagonize HC formation by repressing *Atoh1* expression and ATOH1 activity (Zine et al., 2001, Zheng and Gao, 2000, Li et al., 2008, Doetzlhofer et al., 2009, Tateya et al., 2011).

We recently uncovered that canonical Notch signaling, in addition to its role in HC fate repression, is required for the differentiation and survival of cochlear SCs (Campbell et al., 2016). However, the Notch ligand(s) and receptor(s) involved in this process are

unknown. A potential candidate for instructing SC development is the Notch ligand JAG1. JAG1, which initially is expressed by cochlear and vestibular prosensory progenitors, continues to be highly expressed in SCs (Morrison et al., 1999). While other Notch ligands are down-regulated during the first postnatal week, coinciding with the early phase of cochlear HC and SC maturation, SC-specific JAG1 expression continues throughout adulthood where its function is unknown (Maass et al., 2015, Murata et al., 2006, Hartman et al., 2007, Oesterle et al., 2008).

In the present study, we investigated the role of JAG1 in differentiating and maturing SCs. Our analysis revealed that deletion of *Jag1* at the onset of cochlear differentiation, alters the patterning and cellular morphology of SCs and leads to a down-regulation of genes involved in mitochondrial function and protein synthesis within the sensory epithelium. Furthermore, using morphological analyses and fate-mapping, we show that *Jag1* deletion prior to and after cochlear differentiation resulted in loss of a specialized SC subtype called Hensen cells (HeCs). Functional analysis of adult *Jag1* mutant animals in which *Jag1* was deleted at the perinatal stage revealed mild hearing deficits at low frequencies. Together, our results suggest that *Jag1*-mediated Notch signaling in cochlear SCs is critical for the formation, maintenance, and survival of HeCs.

RESULTS

The mammalian auditory sensory epithelium houses several distinct SC subtypes including HeCs, Deiters' cells (DCs), inner and outer pillar cells (IPCs, OPCs), inner phalangeal cells (IPhCs), and border cells (BCs) (Fig. 1A). To investigate the function of JAG1 in differentiating SCs, we made use of $Jag1^{loxP/loxP}$ ($Jag1^{fx/fx}$) mice, previously

established by Dr. Julian Lewis's group (Brooker et al., 2006) and *Sox2*$^{CreERT2/+}$ mice (Arnold et al., 2011). In the cochlea, *Sox2*$^{CreERT2/+}$ is highly expressed in HC and SC precursors and by one week of age its expression becomes restricted to terminal differentiated SCs (Walters et al., 2015, Gu et al., 2016). We timed-mated *Sox2*$^{CreERT2/+}$*::Jag1*$^{fx/fx}$ with *Jag1*$^{fx/fx}$ mice and administered tamoxifen to pregnant dams at stage embryonic day (E) 14.5 (Fig. 1B), which bypasses the earlier requirement for JAG1 in cochlear prosensory progenitor specification and maintenance (Brooker et al., 2006, Kiernan et al., 2006, Hao et al., 2012, Campbell et al., 2016). To control for *Sox2* haploinsufficiency, we also collected animals that did not receive tamoxifen treatment (untreated). We harvested control (*Jag1*$^{fx/fx}$ treated, *Jag1*$^{fx/fx}$ untreated, and *Sox2*$^{CreERT2/+}$*::Jag1*$^{fx/fx}$ untreated) and *Sox2*$^{CreERT2/+}$*::Jag1*$^{fx/fx}$ treated [*Jag1* conditional knockout (CKO)] embryos at E18.5/postnatal day (P) 0.

First, we analyzed JAG1 expression in control and *Jag1* CKO cochlear tissue to validate Cre-mediated deletion of *Jag1*. In control samples, JAG1 protein was localized at the surface of SCs, except for HeCs (Fig. 1C). By contrast, the majority of SCs in *Jag1* CKO animals lacked JAG1 protein expression (Fig. 1D). Next, we analyzed whether *Jag1* deletion disrupted the formation or patterning of SCs and/or HCs. To label HCs, we used immuno-staining against myosin VIIa, which labels both inner HCs (IHCs) and outer HCs (OHCs) (Hasson et al., 1995). To visualize SCs, we immuno-stained against SOX2, which at E18.5/P0 is highly expressed in the nucleus of all SC subtypes, including HeCs, and is expressed at a lower level in the nucleus of IHCs and OHCs (Kempfle et al., 2016). We found that *Jag1* deletion had no effect on the number (density) of IHCs or OHCs (Fig. 1E, F, I). Our analysis of the SC phenotype, however revealed a significant reduction in the

number of HeCs in *Jag1* CKO mice compared to all three controls (Fig. 1E-I). In cochlear tissue of control animals, $SOX2^{+}$ HeCs were located between the 3rd row of DCs and Claudius cells (CCs), with their nuclei residing in both the HC and SC layers, and with 2-3 HeCs sitting on top of each other (Fig. 1A, E, G). By contrast, *Jag1* CKO cochlear tissue contained either no or only a few scattered HeCs within the HC and SC layers (Fig. 1F, H).

In addition, DCs in *Jag1* CKO mice had enlarged nuclei compared to control mice, and their arrangement appeared to be disorganized, suggesting defects in DC differentiation (Fig. 1G, H). Decreased numbers of DCs in the 2nd and 3rd row (DC2 and DC3) was observed in *Jag1* CKO samples compared to the $Jag1^{fx/fx}$ treated and/or $Jag1^{fx/fx}$ untreated control groups, but not when compared to $Sox2^{CreERT2/+}::Jag1^{fx/fx}$ untreated controls (Fig. 1I). A similar result was observed for IPCs and OPCs (Fig. 1I), suggesting that *Jag1* deficiency combined with *Sox2* haploinsufficiency negatively affects the differentiation of DCs and PCs. Unfortunately, we were unable to address how *Jag1* deficiency combined with *Sox2* haploinsufficiency may impact DC and PC maturation as conditional deletion of *Jag1* at E14.5 resulted in early postnatal lethality. In summary, our analysis demonstrates that JAG1's function is essential for the formation of HeCs in the mammalian cochlea.

To gain insight into how JAG1 may influence HeC development, we characterized JAG1-mediated gene expression changes in the developing auditory sensory epithelium using whole genome micro-arrays. We administered tamoxifen to timed pregnant dams at stage E14.5 and harvested *Jag1* CKO ($Sox2^{CreERT2/+}::Jag1^{fx/fx}$) and control ($Jag1^{fx/fx}$) mice at stage E18.5/P0 (Fig. 2A). We extracted RNA from enzymatically purified control

and *Jag1* CKO cochlear sensory epithelia, and analyzed RNA abundancy using the GeneChip® Mouse Clariom D Arrays (Fig. 2A). Using a one-way ANOVA model we determined genes that were significantly up- (red) or down-regulated (blue) in control versus *Jag1* CKO cochlear epithelial cells. After removing pseudogenes, imprinted, misaligned and low expressing genes (average mean log2 (control, *Jag1* CKO) <5.5), a total of 227 genes were differentially expressed between control and *Jag1* CKO samples with 55 genes being significantly up-regulated (red dots, p-value ≤0.05, log2(FC) ≥3σ) and 172 genes being down-regulated (blue dots, p-value ≤0.05, log2(FC) ≤-3σ) (Fig. 2B). To identify SC-specific genes that are regulated by JAG1-Notch signaling, we utilized published data to generate a high confidence list of 200 SC-specific genes (Maass et al., 2016, Burns et al., 2015). Our analysis revealed that 41 out of these 200 SC-specific genes (21%) were differentially regulated by JAG1-Notch signaling, with 32 being downregulated and 9 being upregulated in *Jag1* CKO samples compared to control (Fig. 2 C) (Supplemental Table 1, 2 genes marked $). Furthermore, the list of down-regulated genes included SC-specific genes previously reported to be positively regulated by Notch signaling (*Agr3*, *F2rl1, Hey1, Igfbp3*, *Lrrtm1, Lsamp*, *Ntf3, Rab3b, Shc3 and Trh*) (Fig. 2B) (Supplemental Table 1, genes marked #) (Maass et al., 2016, Campbell et al., 2016). Conversely, the list of up-regulated genes included a small subset of genes previously shown to be negatively regulated by Notch signaling in response to Notch inhibition (*Cdh4*, *Dpysl2*, *Robo2* and *Cpa6*) (Maass et al., 2016) (Supplemental Table 2, genes marked #). However, deletion of *Jag1* in the differentiating cochlea failed to significantly increase the expression of *Atoh1* or other early HC-specific transcription factors (Supplemental Table 2). This is consistent with our finding that *Jag1* deletion at E14.5

does not result in ectopic HC formation (Fig. 1F, I). To uncover the biological processes associated with JAG1-regulated genes, we performed gene ontology (GO) enrichment analysis using Database for Annotation, Visualization and Integrated Discovery (DAVID). We found that the list of down-regulated genes (p-value ≤0.05, log2(FC) ≤-2σ) was enriched for terms linked to mitochondrial function (oxidative phosphorylation) and mitochondrial dysfunction (Alzheimer, Parkinson and Huntington), as well as protein synthesis (ribosome, intracellular ribonucleoprotein complex) (Fig. 2D, E).

Next, we used qPCR to confirm *Jag1* deletion and validate a subset of SC-specific/enriched genes found to be down-regulated in *Jag1* mutant cochlear epithelia. The genes were selected based on their specific expression in HeCs (*Trpa1*) (Corey et al., 2004), and their association with biological processes of interest including oxidative stress and cell death [*Gpx1* (Ohlemiller et al., 2000), *Apod* (Ganfornina et al., 2008), *Mgst3* (Lu et al., 2016)], mitochondrial inner membrane transport (*Timm13*) (Rothbauer et al., 2001), and prosensory progenitor cell proliferation (*Stox1*) (Nie et al., 2015). We also included in our analysis a subset of genes, that have been reported to be positively regulated by Notch signaling in SC precursors (*Hey1, Igfbp3*) (Campbell et al., 2016) and in SCs (*Hey1*, *Igfbp3*, *Rab3b*) (Maass et al., 2016). We found that *Jag1*, *Hey1*, *Igfbp3*, *Timm13*, *Apod,* and *Trpa1* expression were significantly reduced in *Jag1* mutant cochlear epithelia. *Gpx1*, *Mgst3*, *Rab3b* and *Stox1* expression appeared reduced, but due to variability across samples the reduction was not significant. Taken together, our gene expression analysis confirms the observed defect in HeC formation and suggests a role for JAG1 in tissue homeostasis and metabolism.

In mice, HCs and SCs are not functional at birth and undergo a 2-week long process of postnatal maturation (Legendre et al., 2008, Lelli et al., 2009, Szarama et al., 2012). To address whether JAG1 function is required during postnatal maturation, we deleted *Jag1* after the completion of HC and SC differentiation. To that end, we injected *Jag1* CKO mice and their $Jag1^{fx/fx}$ littermates with 4-hydroxy-tamoxifen at P0/P1. To control for *Sox2* haploinsufficiency, we also collected $Sox2^{CreERT2/+}$::$Jag1^{fx/fx}$ and $Jag1^{fx/fx}$ mice that did not receive 4-hydroxy-tamoxifen treatment (untreated) (Fig. 3A). Control ($Jag1^{fx/fx}$ treated, $Jag1^{fx/fx}$ untreated, and $Sox2^{CreERT2/+}$::$Jag1^{fx/fx}$ untreated) and *Jag1* CKO mice were harvested and analyzed at P5 or P7. JAG1 immuno-staining confirmed the successful deletion of *Jag1* in cochlear tissue obtained from *Jag1* CKO mice (Fig. 3B, C). Next, we quantified HC and SC subtypes at stage P7 in *Jag1* CKO and control mice using the HC and SC markers myosin VIIa and SOX2 respectively. Quantification of SC numbers revealed a significant reduction in the number of HeCs in *Jag1* CKO mice compared to control mice (Fig. 3J). A recent report found that *Sox2* haploinsufficiency at the neonatal stage stimulates PC proliferation and the production of ectopic IHCs (Atkinson et al., 2018). Consistent with these recent findings, quantification of HC numbers in control and *Jag1* CKO mice uncovered a mild increase in the number of IHC in the two groups of mice that contained the $Sox2^{CreERT2/+}$ allele compared to the $Jag1^{fx/fx}$ treated and $Jag1^{fx/fx}$ untreated controls. Also we observed a mild, but significant increase in the number of IPCs in *Jag1* CKO mice compared to $Sox2^{CreERT2/+}$::$Jag1^{fx/fx}$ untreated control animals (Fig 3J).

To confirm the observed HeC loss in *Jag1* CKO mice, we conducted additional experiments, in which we used a combination of fatty acid binding protein 7 (FABP7),

SOX2, and CD44 immuno-staining to distinguish between HeCs, DCs, and CCs. In the postnatal cochlea, FABP7 is highly expressed in the cytoplasm of HeCs, IPhCs, and BCs (Saino-Saito et al., 2010), whereas CD44 is selectively expressed on the cell membranes of OPCs and CCs (Hertzano et al., 2010)(Fig. 3D, D'). In stage P5 control mice, 2-3 HeC nuclei ($SOX2^+$, $FABP7^+$) are stacked on top of each other (Fig. 3F, H), with a single row of HeCs within the SC nuclear layer and a row of stacked HeCs residing in the HC layer (Fig. 3D, D'). By contrast, the cochlea of *Jag1* CKO mice only contained a few scattered $SOX2^+$ HeC-like nuclei within the HC layer and SC layer (Fig. 3E, E'). These HeC-like cells expressed FABP7 at a much-reduced level than HeCs in control mice and some $SOX2^+$ HeC-like cells in *Jag1* CKO mice appeared to co-express CD44, suggesting that these cells may undergo a cell–fate conversion into CCs (Fig. 3E').

To further investigate the HeC-like nuclei with CD44 expression, we performed fate-mapping experiments using $Sox2^{CreERT2/+}::Jag1^{fx/fx}::Rosa26^{tdTomato/+}$ and $Sox2^{CreERT2/+}::Rosa26^{tdTomato/+}$ controls that were injected with tamoxifen at P0/P1 (Fig. 4A). In control samples collected at P7, all $SOX2^+$ SC subtypes, including HeCs, expressed tdTomato (Tom, Fig. 4B, B"), and a small number of $CD44^+$ CCs also expressed Tom (Fig. 4B'). Quantification of Tom^+ cells lateral to the third row of DCs at P7 showed a decrease in the number of Tom^+ cells and Tom^+, $SOX2^+$ cells in all turns of the cochlea when *Jag1* was deleted, which suggests that *Jag1* is important for the survival of some HeCs. In support of these findings, we frequently noted missing cells (Fig. 3G) as well as cellular debris (Fig. 3I) within the HeC region in *Jag1* CKO mice. However, staining with a marker of apoptosis, cleaved caspase-3, revealed no $caspase3^+$ HeCs in the cochlea of *Jag1* CKO mice between P1-P4. There was also a ~2-fold increase in the

number of cells labeled with both Tom and CD44 in *Jag1* CKO cochleae (Fig. 4C-F). Thus, some HeCs appear to lose SOX2 expression and convert into CCs.

To investigate whether *Sox2* haploinsufficiency interacted with *Jag1* deletion to produce changes in HeC numbers, we used a different CreER line to delete *Jag1* from the neonatal cochlea. *Fgfr3-iCreER$^{T2/+}$* is a transgenic allele that has been used extensively in cochlear studies and there have been no reports of haploinsufficiency (Atkinson et al., 2018, Kirjavainen et al., 2015). In contrast with *Sox2$^{CreERT2/+}$* mice, *Fgfr3-iCreER$^{T2/+}$* mice injected with tamoxifen at P0/P1 have CreER expression in ~100% of PCs and DCs, as well as in varying amounts of OHCs depending on the cochlear turn (Cox et al., 2012, McGovern et al., 2017). *Fgfr3-iCreER$^{T2/+}$::Jag1$^{fx/fx}$* and iCre-negative control mice were injected with tamoxifen at P0 and P1 to delete *Jag1*, which was confirmed by RT-PCR showing a second smaller band that lacks exon 4 in *Fgfr3-iCreER$^{T2/+}$::Jag1$^{fx/fx}$* mice (Fig. 5A-B). We quantified HCs and individual SC subtypes at P7 using myosin VIIa to label HCs and SOX2 to label SC nuclei (Fig. 5C-F') and observed a significant loss of HeCs in *Fgfr3-iCreER$^{T2/+}$::Jag1$^{fx/fx}$* mice (Fig. 5I). To confirm that HeCs are missing, we employed two methods: 1) S100a1 immuno-staining to label the cytoplasm and nuclei of PCs and DCs (White et al., 2006, Buckiova and Syka, 2009) and 2) FABP7 immuno-staining to label the cytoplasm of HeCs (Saino-Saito et al., 2010). In control samples, there are two rows of SOX2$^+$, FABP7$^+$ cells located lateral to the S100a1$^+$ third row of DCs (DC3) (Fig. 5E-E', G-G'). However after *Jag1* deletion in *Fgfr3-iCreER$^{T2/+}$::Jag1$^{fx/fx}$* mice, there were no SOX2$^+$ cells located lateral to DC3 cells (Fig. 5F-F', H') and there was a reduction in FABP7 expression (Fig. 5G, H). We also performed immuno-staining with CD44, to label CCs, which are located lateral to HeCs. In *Fgfr3-*

iCreER$^{T2/+}$::Jag1$^{fx/fx}$ mice, the CD44 expression pattern appeared similar to the control, however the CD44 staining was immediately adjacent to the SOX2^{+} DC3 nuclei (Fig. 5G", H"). Together these results confirm that the missing SOX2^{+} cells are HeCs. In addition, there was a slight decrease in the number of OHCs, but no changes in the number of IHCs in *Fgfr3-iCreER$^{T2/+}$::Jag1$^{fx/fx}$* mice at P7 (Fig. 5C-D, I), which rules out the possibility of HeCs converting into HCs. Taken together these results indicate that *Sox2* haploinsufficiency is not responsible for the loss of HeCs after *Jag1* deletion.

We next examined *Fgfr3-iCreER$^{T2/+}$::Jag1$^{fx/fx}$* mice at older ages to investigate whether SC loss progressed to other cell types. After tamoxifen treatment at P0 and P1, the number of HCs and individual SC subtypes were quantified in *Fgfr3-iCreER$^{T2/+}$::Jag1$^{fx/fx}$* cochlea and iCre-negative controls at P30 and P60 (Fig. 6A). Similar to the changes we observed at P7, there was no difference in number of IHCs or OHCs at P30 or P60 compared to the control samples (Fig. 6B-C). For SCs, the only significant difference observed at P30 and P60 was a decrease in HeCs. Thus, neonatal *Jag1* deletion induces HeC loss that occurs by P7 and does not affect other cell types or cause further morphological changes in adulthood.

To assess whether HeC loss affected hearing, we performed auditory brainstem response (ABR) at P30 using *Fgfr3-iCreER$^{T2/+}$::Jag1$^{fx/fx}$* mice and iCre-negative controls that were injected with tamoxifen at P0 and P1 (Fig. 6A). While there was a main effect of genotype, the only significant increase in ABR thresholds in *Fgfr3-iCreER$^{T2/+}$::Jag1$^{fx/fx}$* mice was observed at 4 kHz (Fig. 6D).

To investigate the function of *Jag1* at an older age when HCs and SCs are more mature, we injected *Fgfr3-iCreER$^{T2/+}$::Jag1$^{fx/fx}$* mice with tamoxifen at P6 and P7 and

quantified HCs and individual SC subtypes one week later, at P13 (Fig. 7A). Again, the numbers of IHCs and OHCs remained unchanged (Fig. 7B-D). However, unlike the neonatal *Jag1* deletion that resulted in massive HeC loss across all three cochlear turns, deletion of *Jag1* at P6/P7 induced a mild loss of HeCs that exhibited a gradient across cochlear turns. In the apical turn of *Fgfr3-iCreER$^{T2/+}$::Jag1$^{fx/fx}$* mouse cochleae, no HeC loss was observed (Fig. 7B). In the middle turn, there was a ~20% loss of HeCs (Fig. 7C) and in the basal turn, *Jag1* deletion at P6/P7 caused a larger ~40% loss of HeCs (Fig. 7D). Thus, there appears to be a critical period for *Jag1*'s function in SCs.

DISCUSSION

JAG1 has a well-established role in specifying the prosensory region during development of the inner ear via Notch-mediated lateral induction (Eddison et al., 2000, Brooker et al., 2006, Kiernan et al., 2006, Daudet and Lewis, 2005, Hartman et al., 2010, Neves et al., 2011). However, its expression is maintained in SCs (Murata et al., 2006, Hartman et al., 2007, Oesterle et al., 2008, Maass et al., 2015) without a defined function. Here, we investigated the function of JAG1 in differentiating and maturing cochlea using two complementary *Jag1* CKO mouse models, *Sox2$^{CreERT2/+}$::Jag1$^{fx/fx}$* and *Fgfr3-iCreER$^{T2/+}$::Jag1$^{fx/fx}$*. We show using morphological and fate-mapping analyses that JAG1 is essential for the formation of HeCs and is required for HeC survival and cell fate maintenance during the early phase of cochlear maturation. Furthermore, global gene expression analysis identifies SC-specific genes as *Jag1* targets and reveals a potential link between JAG1-Notch signaling and tissue homeostasis and metabolism. Finally, functional analysis reveals that JAG1 function in the maturing cochlea is critical for low frequency hearing.

Acute disruption of Notch signaling during cochlear differentiation and early maturation triggers the conversion of SC precursors and newly formed SCs into HCs (Yamamoto et al., 2006, Tang et al., 2006, Takebayashi et al., 2007, Doetzlhofer et al., 2009). Thus, it could be reasoned that HeCs are lost due to their conversion into neighboring OHCs. However, our analyses did not reveal any increase in the number of IHCs or OHCs in response to *Jag1* deletion, indicating that JAG1 is dispensable for HC fate repression and that the observed loss of HeCs was not due to their conversion into OHCs.

While Notch signaling is most commonly known for its roles in regulating cell fate and proliferation, recent studies showed that the developing cochlear prosensory cells and later SCs, in particular DCs, depend on Notch signaling for their survival (Yamamoto et al., 2011, Basch et al., 2011, Campbell et al., 2016). Indeed, our analysis uncovered morphological evidence of dead and dying HeCs in P6/7 *Jag1* mutant cochlear tissue and our fate-mapping experiments indicate that approximately one third of HeCs are lost due to cell death. There are several studies demonstrating that Notch signaling promotes the survival of neural stem/progenitor cells (Oishi et al., 2004, Androutsellis-Theotokis et al., 2006, Mason et al., 2006) and tumor cells (Bellavia et al., 2000, Purow et al., 2005). Mechanistic work suggests that Notch activation, through non-canonical pathway(s), activates AKT, NF-κB and mTOR dependent signaling cascades, increasing oxidative metabolism and the expression of pro-survival genes (Oishi et al., 2004, Chan et al., 2007, Perumalsamy et al., 2010, Hossain et al., 2018). Consistent with this link, our gene expression analysis revealed that loss of *Jag1* resulted in a broad down-regulation of genes associated with oxidative phosphorylation and protein synthesis. Future studies

will test the possible role of JAG1 in SC bioenergetics and explore possible links between JAG1-Notch signaling and pro-survival pathways such as AKT-mTOR signaling (Saxton and Sabatini, 2017).

Our fate-mapping experiments also indicate that in response to neonatal *Jag1* deletion, about two thirds of HeCs convert into CD44+, SOX2- CC-like cells. What triggers the up-regulation of CD44 and down-regulation of SOX2 in a subset of HeCs is unclear. JAG1's role in repressing a HeC-to-CC fate switch is reminiscent of its early role in vestibular prosensory cell maintenance. There, JAG1-Notch signaling prevents the conversion of prosensory progenitors into non-sensory cells through maintaining the expression of the transcription factor SOX2 and through antagonizing the transcription factor LMX1A (Mann et al., 2017, Brown et al., 2020). A similar antagonistic relationship between CC-specific determination factors and JAG1-SOX2 axis may be at play and future investigations into the molecular mechanisms of CC fate determination are warranted.

HeCs are a SC subtype located between the 3rd row of DCs and CCs, with no direct contact with HCs. Thus, HeCs may be uniquely vulnerable to *Jag1* deletion since they only receive Notch signals from neighboring DCs through the JAG1 ligand. By contrast the Notch receptors located on DCs and PCs are also activated by the Notch ligands DLL1 and JAG2, expressed by HCs (Lanford et al., 1999; Kiernan et al., 2005; Brooker et al., 2006). Thus *Jag1* deletion using *Sox2*$^{CreERT2/+}$ or *Fgfr3-iCreER*^{T2} removes all Notch signaling from HeCs; whereas DCs and PCs would still receive Notch signaling activated by DLL1 and JAG2. However, HeCs' dependence on JAG1 appears to have a critical period as *Jag1* deletion at P6 produced a less severe phenotype where only 20-

344 40% of HeCs were lost in the middle and basal turns of the cochlea. The milder HeC
345 phenotype at P6 may be due to a lower Cre-mediated recombination efficiency and/or an
346 increase in JAG1 protein stability compared to P0. The later may explain why the apex,
347 which expresses JAG1 at a 2-fold higher levels than other regions of the cochlea, shows
348 no loss of HeCs (Son et al., 2012).

349 *Jag1* deletion at the onset of cochlear differentiation not only resulted in a loss of
350 HeCs but caused mild patterning and laminar structure defects within the auditory sensory
351 epithelium. A recent study proposed that HeCs are involved in the patterning of OHCs
352 during cochlear differentiation. The authors found that HeC division and migration lateral
353 to OHCs produces a shearing motion that facilitates the arrangement of OHCs and DCs
354 into the final checkerboard-like pattern (Cohen et al., 2019). Thus, the mild HC and SC
355 patterning defects we observed may be the result of missing HeCs. Alternatively, the mild
356 defects in cellular patterning in *Jag1* mutant sensory epithelia may be due to altered cell
357 adhesion and/or polarity properties of SCs and HCs.

358 We also observed a decrease in the number of DCs, IPCs, and OPCs when *Jag1*
359 was deleted at E14.5 using $Sox2^{CreERT2/+}$ mice compared to controls that have normal
360 *Sox2* expression, which suggests that loss of JAG1 combined with *Sox2*
361 haploinsufficiency affects DC and PC differentiation. Surprisingly, deletion of *Jag1* at P0
362 using $Sox2^{CreERT2/+}$ mice resulted in an opposite IPC phenotype, with a mild but significant
363 increase in the number of IPCs compared to untreated $Sox2^{CreERT2/+}::Jag1^{fx/fx}$ controls but
364 not compared to controls that have normal *Sox2* expression. These results emphasize
365 the need for controls of various genotypes and the use of different methods to study gene
366 deletions since genes may interact in networks.

We found that *Jag1* deletion at P0 using *Fgfr3-iCreER^{T2}* resulted in mild but significant hearing deficits at 4 kHz. The reason for the decrease in low frequency hearing sensitivity is unknown. However, it is intriguing to speculate that it is causally linked to diminished HeC function. HeCs have a role in the formation of the tectorial membrane (Rau et al., 1999, Kim et al., 2019), they participate in the recycling of potassium ions from the base of OHCs to the endolymph through gap junction connections with DCs (Sato and Santos-Sacchi, 1994, Kikuchi et al., 1995, Zwislocki et al., 1992, Lautermann et al., 1998), and they are involved in maintaining osmotic balance through their expression of aquaporin4 (Takumi et al., 1998, Li and Verkman, 2001). Moreover, a recent study provides evidence that the passive mechanical properties of HeCs may help tune the OHC force generation in the cochlear apex (Gao et al., 2014). Deregulation of any of these processes could alter hearing sensitivity, with the later altering high frequency sensitivity.

While HeCs were discovered over a century ago, little was known about the factors and signals that control their development. In this study, we identify the Notch ligand JAG1 as being essential for HeC differentiation and maturation, revealing a novel role for JAG1 in SC-fate maintenance and SC survival.

MATERIALS AND METHODS

Animals

Sox2$^{CreERT2/+}$ mice (Arnold et al., 2011) (stock #17593) and *Rosa26$^{loxP\text{-}stop\text{-}loxP\text{-}tdTomato}$* (*Rosa26^{tdTomato}*) mice (Madisen et al., 2010) (stock #7914) were purchased from The Jackson Laboratory (Bar Harbor, ME). *Fgfr3-iCreER^{T2}* mice (Rivers et al., 2008, Young et

al., 2010) were provided by Dr. William Richardson (University College, London). Two different *Jag1*$^{fx/fx}$ mouse lines were used in this study. For *Jag1* deletion using *Sox2*$^{CreERT2/+}$ mice, *Jag1*$^{fx/fx}$ mice (Brooker et al., 2006) (MGI: 3623344) were provided by Dr. Julian Lewis (Cancer Research UK London Research Institute). In this line, loxP sites were inserted to flank exons 4 and 5, resulting in a frame shift that generates a stop codon after the start of exon 6 following Cre-mediated recombination. For *Jag1* deletion using *Fgfr3-iCreER*$^{T2/+}$ mice and fate-mapping with *Sox2*$^{CreERT2/+}$ mice, *Jag1*$^{fx/fx}$ mice (Kiernan et al., 2006) (MGI: 3692444) (stock# 10618) were purchased from The Jackson Laboratory (Bar Harbor, ME). In this line, loxP sites were inserted to flank exon 4, resulting in a non-functional JAG1 protein after Cre-mediated recombination. Genotyping was performed in house using PCR as previously described for each line or by Transnetyx, Inc. (Cordova, TN). Mice of both genders were used in all studies. All animal work was performed in accordance with approved animal protocols from the Institutional Animal Care and Use Committees at Johns Hopkins University or Southern Illinois University School of Medicine.

Substances given to animals

Sox2$^{CreERT2/+}$*::Jag1*$^{fx/fx}$ mice: Pregnant dams time-mated to E14.5, received two intraperitoneal (IP) injections of tamoxifen (0.125 mg/g body weight, cat #T5648, Sigma-Aldrich, St. Louis, MO) and progesterone (0.125 mg/g body weight, cat #P3972 Sigma-Aldrich, St. Louis, MO), given 8 hours apart. Neonatal pups were injected with (Z)-4-hydroxytamoxifen (0.139 mg per pup, cat #H7904-5mg, Sigma-Aldrich, St. Louis, MO) at P0 and P1. Controls included Cre-negative littermates, as well as *Sox2*$^{CreERT2/+}$::*Jag1*$^{fx/fx}$

and *Sox2*$^{CreERT2/+}$ mice that did not receive tamoxifen to control for *Sox2* haploinsufficiency. *Fgfr3-iCreER*$^{T2/+}$*::Jag1*$^{fx/fx}$ mice and *Sox2*$^{CreERT2/+}$*::Jag1*$^{fx/fx}$*::Rosa26*^{tdTomato} mice were injected with tamoxifen (0.075mg/g body weight, cat #T5648, Sigma-Aldrich, St. Louis, MO) at P0 and P1, or at P6 and P7. Controls were iCre-negative littermates or *Sox2*$^{CreERT2/+}$*::Rosa26*^{tdTomato} littermates that also received tamoxifen.

Tissue processing

Late embryonic and early postnatal animals were staged using the EMAP eMouse Atlas Project (http://www.emouseatlas.org) Theiler staging criteria. Temporal bones were collected and fixed in 4% paraformaldehyde (PFA, Polysciences, Inc., Warrington, PA) in 10 mM PBS for 2 hours at room temperature. Cochleae were then dissected using the whole mount method as previously described (Montgomery and Cox, 2016). For cryo-sectioning, PFA-fixed inner ears were put through a sucrose gradient (10% sucrose for 30 minutes, 15% sucrose for 30 minutes, and 30% sucrose overnight), submerged in OCT (Tissue-Tek, Sakura Finetek USA, Torrance, CA) and flash frozen. Sections cut at 14 µm thickness were collected on SuperFrost Plus slides (Fisher, Hampton, NH).

Immuno-staining

Cochlear samples were immuno-stained following standard procedures (Montgomery and Cox, 2016). Briefly, tissue was blocked and permeabilized in 10 mM PBS containing 10% Normal Horse Serum (NHS) or Normal Goat Serum (NGS) (Vector Labs, Burlingame, CA), 1% Bovine Serum Albumin (BSA) (Fisher, Hampton, NH), and 1%

Triton-X-100 (Sigma-Aldrich, St. Louis, MO) for 1 hour at room temperature. Then samples were incubated with primary antibodies diluted in 10 mM PBS containing NHS or NGS (5%), BSA (1%), and Triton-X-100 (0.1%) overnight at 4°C or 37°C. The following primary antibodies were used: rabbit anti-FABP7 (1:200, cat #ab32423, Abcam, Cambridge, MA), rat anti-CD44 (1:500, cat #550538, BD Pharmingen, San Jose, CA), rabbit anti-cleaved caspase3 (1:1000, cat #9661, Cell Signaling Technology, Danvers, MA), goat anti-JAG1 (1:500, cat #sc-6011, Santa Cruz Biotechnology, Dallas, TX), rabbit anti-myosin VIIa (1:200, cat #25-6790, Proteus BioSciences, Ramona, CA), mouse anti-parvalbumin (1:1000, cat #P3088, Sigma-Aldrich, St. Louis, MO), rabbit anti-S100a1 (1:400, cat #ab868, Abcam, Cambridge, MA), and goat anti-SOX2 (1:400, cat #sc-17320, Santa Cruz Biotechnology, Dallas, TX). The next day, samples were incubated in corresponding Alexa Fluor-conjugated secondary antibodies (1:1000, Life Technologies, Eugene, OR) for 2 hours at room temperature. Nuclei were stained with Hoechst 33342 (1:2000, cat #H1399, Fisher, Hampton, NH) for 20 minutes at room temperature, followed by mounting on slides in Prolong Gold (cat #P36930, Fisher, Hampton, NH). To increase the signal to noise ratio, some samples stained with anti-SOX2 antibodies were pretreated with signal enhancer (cat #136933, Life Technologies, Eugene, OR) for 30 min at room temperature before the blocking and permeabilization step. Samples were imaged using a Zeiss LSM 800 confocal microscope and processed with Zen Blue and ZEN 2.3 SP1 software (Carl Zeiss, Oberkochen, Germany).

Cell counts

Confocal z-stacks through the HC layer and corresponding SC layer were taken at two representative regions in each turn of the cochlear (apex, middle, and base). Labeled IHCs, OHCs, and different SC subtypes were quantified in two 150 or 200 μm representative regions in each turn of the cochlea. The length of the imaged segment (150 or 250 μm) was analyzed using Image J (http://imagej.nih.gov/ij) or Zen Blue software. HCs and SCs were manually counted in Photoshop CS5 (Adobe, San Jose, CA) or in Zen Blue software.

Validation of *Jag1* deletion

Immuno-staining with anti-JAG1 antibodies was used to validate deletion of *Jag1* from SCs using the *Jag1*$^{fx/fx}$ allele that was provided by Dr. Julian Lewis (Brooker et al., 2006). However, the *Jag1*$^{fx/fx}$ allele purchased from The Jackson Laboratories produces a truncated protein that was still detected by anti-JAG1 antibodies. Therefore, we used RT-PCR to validate the deletion of *Jag1* from SCs in these mice. Total RNA was extracted from P7 *Jag1*$^{fx/fx}$ and *Fgfr3-iCreER*$^{T2/+}$*::Jag1*$^{fx/fx}$ cochleae using tri-reagent (cat #T9424, Sigma-Aldrich, St. Louis, MO). RNA was then precipitated with isopropanol (cat #327930010, Acros Organics, Geel, Belgium) overnight at -20˚C, purified with DNAse treatment (cat #AM1906, Fisher, Hampton, NH) and re-precipitated with sodium acetate (cat #BP333, Fisher, Hampton, NH). Reverse transcription into cDNA was performed using Thermo Scientific Maxima First Strand cDNA synthesis kit (cat #K1641, Fisher, Hampton, NH, United States). cDNA was amplified with primers that flanked exon 4 of *Jag1* [forward: CGA CCG TAA TCG CAT CGT AC, reverse: AGT CCC ACA GTA ATT CAG ATC; (Kiernan et al., 2006)], separated on a 1% agarose gel and visualized with

GelRed nucleic acid stain (cat #41001, Biotium, Fremont, CA) using a Syngene G:Box Chemi imager (Syngene, Frederick, MD).

Microarray and RT-qPCR experiments

For microarray and qPCR validation experiments control (*Jag1*$^{fx/fx}$) and experimental animals (*Sox2*$^{CreERT2/+}$*::Jag1*$^{fx/fx}$) were harvested at P0 after receiving tamoxifen and progesterone at stage E14.5. Cochlear epithelia from individual animals were isolated using dispase/collagenase digest as previously described (Doetzlhofer et al., 2009). Total RNA was extracted using the RNeasy Micro Kit (cat #74004, QIAGEN, Germantown, MD). For the microarray experiment, total RNA was labeled with the Affymetrix GeneChip WT PLUS Reagent Kit using the manufacturer's protocol. Labeled RNA was hybridized onto Clariom D mouse microarray (Affymetrix, Santa Clara, CA) and chips were scanned and analyzed according to manufacturer's manuals. Affymetrix CEL files were extracted and data normalized with the Partek GS 6.6 platform (Partek Inc., Chesterfield, MO). Partek's extended meta-probe set was used with RMA normalization to create quantile-normalized log2 transcript signal values, which were used in subsequent ANOVA analyses. The microarray data is deposited in the Gene Expression Omnibus (GEO) data base, accession number GSE148009. Results were validated using qPCR experiments where mRNA was reverse transcribed into cDNA using the iScript cDNA synthesis kit (cat #1708891, Bio-Rad, Hercules, CA). SYBR Green based qPCR was performed on a CFX-Connect Real Time PCR Detection System (Bio-Rad, Hercules, CA) using Fast SYBR® Green Master Mix reagent (cat #4385616, Applied Biosystems, Foster City, CA) and gene-specific primers. Relative gene expression was analyzed using the comparative CT

method (Schmittgen and Livak, 2008). The ribosomal gene *Rpl19* was used as reference gene and wild-type early postnatal cochlear tissue was used as calibrator. The following qPCR primers were used:

Gene	Forward Primer	Reverse Primer
Apod	*GGCTTCAACGGTGTTTGTTT*	*GAGGGTGGGATGTTCTCTGA*
Gpx1	*GTCCACCGTGTATGCCTTCT*	*CTCCTGGTGTCCGAACTGAT*
Hey1	*CACTGCAGGAGGGAAAGGTTAT*	*CCCCAAACTCCGATAGTCCAT*
Igfbp3	*AACCTGCTCCAGGAAACATCAGT*	*GCTTTCCACACTCCCAGCAT*
Jag1	*TGTGCAAACATCACTTTCACCTTT*	*GCAAATGTGTTCGGTGGTAAGAC*
Mgst3	*TGAGAACGGGCATATGTTCA*	*GCTTGCTAGGGTCTCCTGTG*
Rab3b	*TTCCGCTATGCTGATGACAC*	*CCACGGTAGTAGGCTGTGGT*
Rpl19	*GGTCTGGTTGGATCCCAATG*	*CCCGGGAATGGACAGTCA*
Stox1	*TGCACGCAGAGGATAAGACA*	*CACTGTGACTCAAAGCCACC*
Timm13	*GCCATTATGGAGCAGGTGAA*	*CGCTGCAGTCGAGAGTTGTA*
Trpa1	*AACACGGCTTTGATGTCCAC*	*GGGCTGGCTTTCTTGTGATT*

Gene Ontology Analysis

Gene ontology (GO) enrichment analysis was conducted using the Functional Annotation Tool in DAVID (Huang da et al., 2009b, Huang da et al., 2009a). A curated list of down-regulated genes (p-value ≤0.05, log2 (FC) ≤ -2σ, mean log2 Ctrl ≥5) was uploaded into the DAVID bioinformatics suite 6.8 and GO terms related to biological process (GOTERM BP DIRECT), molecular function (GOTERM MF DIRECT), cellular compartment (GOTERM CC DIRECT), and KEGG pathway term (KEGG PATHWAY) were obtained using default parameters.

Auditory brainstem response (ABR) measurements

To assess hearing after *Jag1* deletion, ABR was measured at P30 in *Fgfr3-iCreER*$^{T2/+}$*::Jag1*$^{fx/fx}$ mice and iCre-negative littermates injected with tamoxifen at P0/P1. Before ABR recordings, mice were anesthetized with Avertin (250-500mg/kg, IP, Sigma-Aldrich, St. Louis, MO), and kept on a heating pad in a sound attenuated booth (Industrial Acoustic, Bronx, NY) throughout the whole procedure. One subdermal stainless-steel recording electrode was inserted at the vertex of the skull, with a second reference electrode inserted under the pinna of the left ear. A ground electrode was inserted at the base of the tail. An electrostatic speaker (EC1, Tucker Davis Technologies [TDT] System III, TDT, Alachua, FL) was fitted to a tube and inserted into the left ear canal. Acoustic signals were generated using a 16-bit D/A converter (RX6, TDT System III, TDT, Alachua, FL), controlled by a customized Auditory Neurophysiology Experiment Control Software (ANECS, Blue Hills Scientific, Boston, MA). To generate ABRs, pure tone bursts at 4, 8, 12, 16, and 22 kHz were presented at a rate of 19/sec, with a 5 ms duration, and repeated 512 times. Sound intensity at each frequency decreased from 80 to 5 dB, with 5 dB steps. Two blinded reviewers determined the ABR thresholds, which were the lowest sound intensity that produced a visually distinct response in wave I or II.

Statistical Analysis

The sample size (n) represents the number of animals analyzed per group. Animals (biological replicates) were allocated into control or experimental groups based on genotype and/or type of treatment. To avoid bias, masking was used during data analysis.

P-values ≤ 0.05 were considered significant. Data was analyzed using Graphpad Prism 6.02 and 8.0 (Graphpad Software Inc., La Jolla, CA).

ACKNOWLEDGEMENTS

We thank Dr. William Richardson at University College London for providing the *Fgfr3-iCreER*^{T2} mouse line, and Dr. Julian Lewis at Cancer Research UK London Research Institute for providing one of the *Jag1*$^{fx/fx}$ mouse lines. This work was supported by grants from NIDCD [R01DC011571 (AD) and R01DC014441 (BC)] and the Office of the Assistant Secretary of Defense for Health Affairs [W81XWH-15-1-0475 (BC)]. The Southern Illinois University School of Medicine Research Imaging Facility is supported by a grant from the Office of Naval Research (N00014-15-1-2866).

COMPETING INTERESTS

Brandon C. Cox, PhD is a consultant for Turner Scientific, LLC, and Otonomy, Inc.

Other authors do not have anything to declare.

REFERENCES

ADAM, J., MYAT, A., LE ROUX, I., EDDISON, M., HENRIQUE, D., ISH-HOROWICZ, D. & LEWIS, J. 1998. Cell fate choices and the expression of Notch, Delta and Serrate homologues in the chick inner ear: parallels with Drosophila sense-organ development. *Development,* 125**,** 4645-54.

ANDROUTSELLIS-THEOTOKIS, A., LEKER, R. R., SOLDNER, F., HOEPPNER, D. J., RAVIN, R., POSER, S. W., RUEGER, M. A., BAE, S. K., KITTAPPA, R. & MCKAY, R. D. 2006. Notch signalling regulates stem cell numbers in vitro and in vivo. *Nature,* 442**,** 823-6.

ARNOLD, K., SARKAR, A., YRAM, M. A., POLO, J. M., BRONSON, R., SENGUPTA, S., SEANDEL, M., GEIJSEN, N. & HOCHEDLINGER, K. 2011. Sox2(+) adult stem and progenitor cells are important for tissue regeneration and survival of mice. *Cell Stem Cell,* 9**,** 317-29.

ATKINSON, P. J., DONG, Y., GU, S., LIU, W., NAJARRO, E. H., UDAGAWA, T. & CHENG, A. G. 2018. Sox2 haploinsufficiency primes regeneration and Wnt responsiveness in the mouse cochlea. *J Clin Invest,* 128**,** 1641-1656.

BASCH, M. L., OHYAMA, T., SEGIL, N. & GROVES, A. K. 2011. Canonical Notch signaling is not necessary for prosensory induction in the mouse cochlea: insights from a conditional mutant of RBPjkappa. *J Neurosci,* 31**,** 8046-58.

BELLAVIA, D., CAMPESE, A. F., ALESSE, E., VACCA, A., FELLI, M. P., BALESTRI, A., STOPPACCIARO, A., TIVERON, C., TATANGELO, L., GIOVARELLI, M., GAETANO, C., RUCO, L., HOFFMAN, E. S., HAYDAY, A. C., LENDAHL, U., FRATI, L., GULINO, A. & SCREPANTI, I. 2000. Constitutive activation of NF-kappaB and T-cell leukemia/lymphoma in Notch3 transgenic mice. *EMBO J,* 19**,** 3337-48.

BERMINGHAM, N. A., HASSAN, B. A., PRICE, S. D., VOLLRATH, M. A., BEN-ARIE, N., EATOCK, R. A., BELLEN, H. J., LYSAKOWSKI, A. & ZOGHBI, H. Y. 1999. Math1: an essential gene for the generation of inner ear hair cells. *Science,* 284**,** 1837-41.

BROOKER, R., HOZUMI, K. & LEWIS, J. 2006. Notch ligands with contrasting functions: Jagged1 and Delta1 in the mouse inner ear. *Development,* 133**,** 1277-86.

BROWN, R. M., 2ND, NELSON, J. C., ZHANG, H., KIERNAN, A. E. & GROVES, A. K. 2020. Notch-mediated lateral induction is necessary to maintain vestibular prosensory identity during inner ear development. *Dev Biol*.

BUCKIOVA, D. & SYKA, J. 2009. Calbindin and S100 protein expression in the developing inner ear in mice. *J Comp Neurol,* 513**,** 469-82.

BURNS, J. C., KELLY, M. C., HOA, M., MORELL, R. J. & KELLEY, M. W. 2015. Single-cell RNA-Seq resolves cellular complexity in sensory organs from the neonatal inner ear. *Nat Commun,* 6**,** 8557.

CAMPBELL, D. P., CHRYSOSTOMOU, E. & DOETZLHOFER, A. 2016. Canonical Notch signaling plays an instructive role in auditory supporting cell development. *Sci Rep,* 6**,** 19484.

CHAN, S. M., WENG, A. P., TIBSHIRANI, R., ASTER, J. C. & UTZ, P. J. 2007. Notch signals positively regulate activity of the mTOR pathway in T-cell acute lymphoblastic leukemia. *Blood,* 110**,** 278-86.

CHEN, P., JOHNSON, J. E., ZOGHBI, H. Y. & SEGIL, N. 2002. The role of Math1 in inner ear development: Uncoupling the establishment of the sensory primordium from hair cell fate determination. *Development,* 129**,** 2495-505.

COHEN, R., AMIR-ZILBERSTEIN, L., HERSCH, M., WOLAND, S., TAIBER, S., MATSUZAKI, F., BERGMANN, S., AVRAHAM, K. & SPRINZAK, D. 2019. Shear forces drive precise patterning of hair cells in the mammalian inner ear. bioRxiv.

COREY, D. P., GARCIA-ANOVEROS, J., HOLT, J. R., KWAN, K. Y., LIN, S. Y., VOLLRATH, M. A., AMALFITANO, A., CHEUNG, E. L., DERFLER, B. H., DUGGAN, A., GELEOC, G. S., GRAY, P. A., HOFFMAN, M. P., REHM, H. L., TAMASAUSKAS, D. & ZHANG, D. S. 2004. TRPA1 is a candidate for the mechanosensitive transduction channel of vertebrate hair cells. *Nature,* 432**,** 723-30.

COX, B. C., LIU, Z., LAGARDE, M. M. & ZUO, J. 2012. Conditional gene expression in the mouse inner ear using Cre-loxP. *J Assoc Res Otolaryngol,* 13**,** 295-322.

DAUDET, N. & LEWIS, J. 2005. Two contrasting roles for Notch activity in chick inner ear development: specification of prosensory patches and lateral inhibition of hair-cell differentiation. *Development,* 132**,** 541-51.

DAUDET, N. & ZAK, M. 2020. Notch Signalling: The Multitask Manager of Inner Ear Development and Regeneration. *Adv Exp Med Biol,* 1218**,** 129-157.

DOETZLHOFER, A., BASCH, M. L., OHYAMA, T., GESSLER, M., GROVES, A. K. & SEGIL, N. 2009. Hey2 regulation by FGF provides a Notch-independent mechanism for maintaining pillar cell fate in the organ of Corti. *Dev Cell,* 16**,** 58-69.

EDDISON, M., LE ROUX, I. & LEWIS, J. 2000. Notch signaling in the development of the inner ear: lessons from Drosophila. *Proc Natl Acad Sci U S A,* 97**,** 11692-9.

GANFORNINA, M. D., DO CARMO, S., LORA, J. M., TORRES-SCHUMANN, S., VOGEL, M., ALLHORN, M., GONZALEZ, C., BASTIANI, M. J., RASSART, E. & SANCHEZ, D. 2008. Apolipoprotein D is involved in the mechanisms regulating protection from oxidative stress. *Aging Cell,* 7**,** 506-15.

GAO, S. S., WANG, R., RAPHAEL, P. D., MOAYEDI, Y., GROVES, A. K., ZUO, J., APPLEGATE, B. E. & OGHALAI, J. S. 2014. Vibration of the organ of Corti within the cochlear apex in mice. *J Neurophysiol,* 112**,** 1192-204.

GU, R., BROWN, R. M., 2ND, HSU, C. W., CAI, T., CROWDER, A. L., PIAZZA, V. G., VADAKKAN, T. J., DICKINSON, M. E. & GROVES, A. K. 2016. Lineage tracing of Sox2-expressing progenitor cells in the mouse inner ear reveals a broad contribution to non-sensory tissues and insights into the origin of the organ of Corti. *Dev Biol,* 414**,** 72-84.

HAO, J., KOESTERS, R., BOUCHARD, M., GRIDLEY, T., PFANNENSTIEL, S., PLINKERT, P. K., ZHANG, L. & PRAETORIUS, M. 2012. Jagged1-mediated Notch signaling regulates mammalian inner ear development independent of lateral inhibition. *Acta Otolaryngol,* 132**,** 1028-35.

HARTMAN, B. H., HAYASHI, T., NELSON, B. R., BERMINGHAM-MCDONOGH, O. & REH, T. A. 2007. Dll3 is expressed in developing hair cells in the mammalian cochlea. *Dev Dyn,* 236**,** 2875-83.

HARTMAN, B. H., REH, T. A. & BERMINGHAM-MCDONOGH, O. 2010. Notch signaling specifies prosensory domains via lateral induction in the developing mammalian inner ear. *Proc Natl Acad Sci U S A,* 107**,** 15792-7.

HASSON, T., HEINTZELMAN, M. B., SANTOS-SACCHI, J., COREY, D. P. & MOOSEKER, M. S. 1995. Expression in cochlea and retina of myosin VIIa, the gene product defective in Usher syndrome type 1B. *Proc Natl Acad Sci U S A,* 92**,** 9815-9.

HERTZANO, R., PULIGILLA, C., CHAN, S. L., TIMOTHY, C., DEPIREUX, D. A., AHMED, Z., WOLF, J., EISENMAN, D. J., FRIEDMAN, T. B., RIAZUDDIN, S., KELLEY, M. W. & STROME, S. E. 2010. CD44 is a marker for the outer pillar cells in the early postnatal mouse inner ear. *J Assoc Res Otolaryngol,* 11**,** 407-18.

HOSSAIN, F., SORRENTINO, C., UCAR, D. A., PENG, Y., MATOSSIAN, M., WYCZECHOWSKA, D., CRABTREE, J., ZABALETA, J., MORELLO, S., DEL VALLE, L., BUROW, M., COLLINS-BUROW, B., PANNUTI, A., MINTER, L. M., GOLDE, T. E., OSBORNE, B. A. & MIELE, L. 2018. Notch Signaling Regulates Mitochondrial Metabolism and NF-kappaB Activity in Triple-Negative Breast Cancer Cells via IKKalpha-Dependent Non-canonical Pathways. *Front Oncol,* 8**,** 575.

HUANG DA, W., SHERMAN, B. T. & LEMPICKI, R. A. 2009a. Bioinformatics enrichment tools: paths toward the comprehensive functional analysis of large gene lists. *Nucleic Acids Res,* 37**,** 1-13.

HUANG DA, W., SHERMAN, B. T. & LEMPICKI, R. A. 2009b. Systematic and integrative analysis of large gene lists using DAVID bioinformatics resources. *Nat Protoc,* 4**,** 44-57.

KEMPFLE, J. S., TURBAN, J. L. & EDGE, A. S. 2016. Sox2 in the differentiation of cochlear progenitor cells. *Sci Rep,* 6**,** 23293.

KIERNAN, A. E., CORDES, R., KOPAN, R., GOSSLER, A. & GRIDLEY, T. 2005. The Notch ligands DLL1 and JAG2 act synergistically to regulate hair cell development in the mammalian inner ear. *Development,* 132**,** 4353-62.

KIERNAN, A. E., XU, J. & GRIDLEY, T. 2006. The Notch ligand JAG1 is required for sensory progenitor development in the mammalian inner ear. *PLoS Genet,* 2**,** e4.

KIKUCHI, T., KIMURA, R. S., PAUL, D. L. & ADAMS, J. C. 1995. Gap junctions in the rat cochlea: immunohistochemical and ultrastructural analysis. *Anat Embryol (Berl),* 191**,** 101-18.

KIM, D. K., KIM, J. A., PARK, J., NIAZI, A., ALMISHAAL, A. & PARK, S. 2019. The release of surface-anchored alpha-tectorin, an apical extracellular matrix protein, mediates tectorial membrane organization. *Sci Adv,* 5**,** eaay6300.

KIRJAVAINEN, A., LAOS, M., ANTTONEN, T. & PIRVOLA, U. 2015. The Rho GTPase Cdc42 regulates hair cell planar polarity and cellular patterning in the developing cochlea. *Biol Open,* 4**,** 516-26.

KOPAN, R. & ILAGAN, M. X. 2009. The canonical Notch signaling pathway: unfolding the activation mechanism. *Cell,* 137**,** 216-33.

LANFORD, P. J., LAN, Y., JIANG, R., LINDSELL, C., WEINMASTER, G., GRIDLEY, T. & KELLEY, M. W. 1999. Notch signalling pathway mediates hair cell development in mammalian cochlea. *Nat Genet,* 21**,** 289-92.

LAUTERMANN, J., TEN CATE, W. J., ALTENHOFF, P., GRUMMER, R., TRAUB, O., FRANK, H., JAHNKE, K. & WINTERHAGER, E. 1998. Expression of the gap-junction connexins 26 and 30 in the rat cochlea. *Cell Tissue Res,* 294**,** 415-20.

LEGENDRE, K., SAFIEDDINE, S., KUSSEL-ANDERMANN, P., PETIT, C. & EL-AMRAOUI, A. 2008. alphaII-betaV spectrin bridges the plasma membrane and cortical lattice in the lateral wall of the auditory outer hair cells. *J Cell Sci,* 121**,** 3347-56.

LELLI, A., ASAI, Y., FORGE, A., HOLT, J. R. & GELEOC, G. S. 2009. Tonotopic gradient in the developmental acquisition of sensory transduction in outer hair cells of the mouse cochlea. *J Neurophysiol,* 101**,** 2961-73.

LI, J. & VERKMAN, A. S. 2001. Impaired hearing in mice lacking aquaporin-4 water channels. *J Biol Chem,* 276**,** 31233-7.

LI, S., MARK, S., RADDE-GALLWITZ, K., SCHLISNER, R., CHIN, M. T. & CHEN, P. 2008. Hey2 functions in parallel with Hes1 and Hes5 for mammalian auditory sensory organ development. *BMC Dev Biol,* 8**,** 20.

LU, L., PANDEY, A. K., HOUSEAL, M. T. & MULLIGAN, M. K. 2016. The Genetic Architecture of Murine Glutathione Transferases. *PLoS One,* 11**,** e0148230.

MAASS, J. C., GU, R., BASCH, M. L., WALDHAUS, J., LOPEZ, E. M., XIA, A., OGHALAI, J. S., HELLER, S. & GROVES, A. K. 2015. Changes in the regulation of the Notch signaling pathway are temporally correlated with regenerative failure in the mouse cochlea. *Front Cell Neurosci,* 9**,** 110.

MAASS, J. C., GU, R., CAI, T., WAN, Y. W., CANTELLANO, S. C., ASPRER, J. S., ZHANG, H., JEN, H. I., EDLUND, R. K., LIU, Z. & GROVES, A. K. 2016. Transcriptomic Analysis of Mouse Cochlear Supporting Cell Maturation Reveals Large-Scale Changes in Notch Responsiveness Prior to the Onset of Hearing. *PLoS One,* 11**,** e0167286.

MADISEN, L., ZWINGMAN, T. A., SUNKIN, S. M., OH, S. W., ZARIWALA, H. A., GU, H., NG, L. L., PALMITER, R. D., HAWRYLYCZ, M. J., JONES, A. R., LEIN, E. S. & ZENG, H. 2010. A robust and high-throughput Cre reporting and characterization system for the whole mouse brain. *Nat Neurosci,* 13**,** 133-40.

MANN, Z. F., GALVEZ, H., PEDRENO, D., CHEN, Z., CHRYSOSTOMOU, E., ZAK, M., KANG, M., CANDEN, E. & DAUDET, N. 2017. Shaping of inner ear sensory organs through antagonistic interactions between Notch signalling and Lmx1a. *Elife,* 6.

MASON, H. A., RAKOWIECKI, S. M., GRIDLEY, T. & FISHELL, G. 2006. Loss of notch activity in the developing central nervous system leads to increased cell death. *Dev Neurosci,* 28**,** 49-57.

MCGOVERN, M. M., BRANCHECK, J., GRANT, A. C., GRAVES, K. A. & COX, B. C. 2017. Quantitative Analysis of Supporting Cell Subtype Labeling Among CreER Lines in the Neonatal Mouse Cochlea. *J Assoc Res Otolaryngol,* 18**,** 227-245.

MONTGOMERY, S. C. & COX, B. C. 2016. Whole Mount Dissection and Immunofluorescence of the Adult Mouse Cochlea. *J Vis Exp*.

MORRISON, A., HODGETTS, C., GOSSLER, A., HRABE DE ANGELIS, M. & LEWIS, J. 1999. Expression of Delta1 and Serrate1 (Jagged1) in the mouse inner ear. *Mech Dev,* 84**,** 169-72.

MURATA, J., TOKUNAGA, A., OKANO, H. & KUBO, T. 2006. Mapping of notch activation during cochlear development in mice: implications for determination of prosensory domain and cell fate diversification. *J Comp Neurol,* 497**,** 502-18.

NEVES, J., PARADA, C., CHAMIZO, M. & GIRALDEZ, F. 2011. Jagged 1 regulates the restriction of Sox2 expression in the developing chicken inner ear: a mechanism for sensory organ specification. *Development,* 138**,** 735-44.

NIE, X., ZHANG, K., WANG, L., OU, G., ZHU, H. & GAO, W. Q. 2015. Transcription factor STOX1 regulates proliferation of inner ear epithelial cells via the AKT pathway. *Cell Prolif,* 48**,** 209-20.

OESTERLE, E. C., CAMPBELL, S., TAYLOR, R. R., FORGE, A. & HUME, C. R. 2008. Sox2 and JAGGED1 expression in normal and drug-damaged adult mouse inner ear. *J Assoc Res Otolaryngol,* 9**,** 65-89.

OHLEMILLER, K. K., MCFADDEN, S. L., DING, D. L., LEAR, P. M. & HO, Y. S. 2000. Targeted mutation of the gene for cellular glutathione peroxidase (Gpx1) increases noise-induced hearing loss in mice. *J Assoc Res Otolaryngol,* 1**,** 243-54.

OISHI, K., KAMAKURA, S., ISAZAWA, Y., YOSHIMATSU, T., KUIDA, K., NAKAFUKU, M., MASUYAMA, N. & GOTOH, Y. 2004. Notch promotes survival of neural precursor cells via mechanisms distinct from those regulating neurogenesis. *Dev Biol,* 276**,** 172-84.

PAN, W., JIN, Y., STANGER, B. & KIERNAN, A. E. 2010. Notch signaling is required for the generation of hair cells and supporting cells in the mammalian inner ear. *Proc Natl Acad Sci U S A,* 107**,** 15798-803.

PERUMALSAMY, L. R., NAGALA, M. & SARIN, A. 2010. Notch-activated signaling cascade interacts with mitochondrial remodeling proteins to regulate cell survival. *Proc Natl Acad Sci U S A,* 107**,** 6882-7.

PETROVIC, J., FORMOSA-JORDAN, P., LUNA-ESCALANTE, J. C., ABELLO, G., IBANES, M., NEVES, J. & GIRALDEZ, F. 2014. Ligand-dependent Notch signaling strength orchestrates lateral induction and lateral inhibition in the developing inner ear. *Development,* 141**,** 2313-24.

PUROW, B. W., HAQUE, R. M., NOEL, M. W., SU, Q., BURDICK, M. J., LEE, J., SUNDARESAN, T., PASTORINO, S., PARK, J. K., MIKOLAENKO, I., MARIC, D., EBERHART, C. G. & FINE, H. A. 2005. Expression of Notch-1 and its ligands, Delta-like-1 and Jagged-1, is critical for glioma cell survival and proliferation. *Cancer Res,* 65**,** 2353-63.

RAU, A., LEGAN, P. K. & RICHARDSON, G. P. 1999. Tectorin mRNA expression is spatially and temporally restricted during mouse inner ear development. *J Comp Neurol,* 405**,** 271-80.

RIVERS, L. E., YOUNG, K. M., RIZZI, M., JAMEN, F., PSACHOULIA, K., WADE, A., KESSARIS, N. & RICHARDSON, W. D. 2008. PDGFRA/NG2 glia generate myelinating oligodendrocytes and piriform projection neurons in adult mice. *Nat Neurosci,* 11**,** 1392-401.

ROTHBAUER, U., HOFMANN, S., MUHLENBEIN, N., PASCHEN, S. A., GERBITZ, K. D., NEUPERT, W., BRUNNER, M. & BAUER, M. F. 2001. Role of the deafness dystonia peptide 1 (DDP1) in import of human Tim23 into the inner membrane of mitochondria. *J Biol Chem,* 276**,** 37327-34.

SAINO-SAITO, S., SUZUKI, R., TOKUDA, N., ABE, H., KONDO, H. & OWADA, Y. 2010. Localization of fatty acid binding proteins (FABPs) in the cochlea of mice. *Ann Anat,* 192**,** 210-4.

SATO, Y. & SANTOS-SACCHI, J. 1994. Cell coupling in the supporting cells of Corti's organ: sensitivity to intracellular H+ and Ca+2. *Hear Res,* 80**,** 21-4.

SAXTON, R. A. & SABATINI, D. M. 2017. mTOR Signaling in Growth, Metabolism, and Disease. *Cell,* 169**,** 361-371.

SCHMITTGEN, T. D. & LIVAK, K. J. 2008. Analyzing real-time PCR data by the comparative C(T) method. *Nat Protoc,* 3**,** 1101-8.

SON, E. J., WU, L., YOON, H., KIM, S., CHOI, J. Y. & BOK, J. 2012. Developmental gene expression profiling along the tonotopic axis of the mouse cochlea. *PLoS One,* 7**,** e40735.

SZARAMA, K. B., GAVARA, N., PETRALIA, R. S., KELLEY, M. W. & CHADWICK, R. S. 2012. Cytoskeletal changes in actin and microtubules underlie the developing surface mechanical properties of sensory and supporting cells in the mouse cochlea. *Development,* 139**,** 2187-97.

TAKEBAYASHI, S., YAMAMOTO, N., YABE, D., FUKUDA, H., KOJIMA, K., ITO, J. & HONJO, T. 2007. Multiple roles of Notch signaling in cochlear development. *Dev Biol,* 307**,** 165-78.

TAKUMI, Y., NAGELHUS, E. A., EIDET, J., MATSUBARA, A., USAMI, S., SHINKAWA, H., NIELSEN, S. & OTTERSEN, O. P. 1998. Select types of supporting cell in the inner ear express aquaporin-4 water channel protein. *Eur J Neurosci,* 10**,** 3584-95.

TANG, L. S., ALGER, H. M. & PEREIRA, F. A. 2006. COUP-TFI controls Notch regulation of hair cell and support cell differentiation. *Development,* 133**,** 3683-93.

TATEYA, T., IMAYOSHI, I., TATEYA, I., ITO, J. & KAGEYAMA, R. 2011. Cooperative functions of Hes/Hey genes in auditory hair cell and supporting cell development. *Dev Biol,* 352**,** 329-40.

WALTERS, B. J., YAMASHITA, T. & ZUO, J. 2015. Sox2-CreER mice are useful for fate mapping of mature, but not neonatal, cochlear supporting cells in hair cell regeneration studies. *Sci Rep,* 5**,** 11621.

WHITE, P. M., DOETZLHOFER, A., LEE, Y. S., GROVES, A. K. & SEGIL, N. 2006. Mammalian cochlear supporting cells can divide and trans-differentiate into hair cells. *Nature,* 441**,** 984-7.

WOODS, C., MONTCOUQUIOL, M. & KELLEY, M. W. 2004. Math1 regulates development of the sensory epithelium in the mammalian cochlea. *Nat Neurosci,* 7**,** 1310-8.

YAMAMOTO, N., CHANG, W. & KELLEY, M. W. 2011. Rbpj regulates development of prosensory cells in the mammalian inner ear. *Dev Biol,* 353**,** 367-79.

YAMAMOTO, N., TANIGAKI, K., TSUJI, M., YABE, D., ITO, J. & HONJO, T. 2006. Inhibition of Notch/RBP-J signaling induces hair cell formation in neonate mouse cochleas. *J Mol Med (Berl),* 84**,** 37-45.

YOUNG, K. M., MITSUMORI, T., PRINGLE, N., GRIST, M., KESSARIS, N. & RICHARDSON, W. D. 2010. An Fgfr3-iCreER(T2) transgenic mouse line for studies of neural stem cells and astrocytes. *Glia,* 58**,** 943-53.

ZHENG, J. L. & GAO, W. Q. 2000. Overexpression of Math1 induces robust production of extra hair cells in postnatal rat inner ears. *Nat Neurosci,* 3**,** 580-6.

ZINE, A., AUBERT, A., QIU, J., THERIANOS, S., GUILLEMOT, F., KAGEYAMA, R. & DE RIBAUPIERRE, F. 2001. Hes1 and Hes5 activities are required for the normal development of the hair cells in the mammalian inner ear. *J Neurosci,* 21**,** 4712-20.

ZWISLOCKI, J. J., SLEPECKY, N. B., CEFARATTI, L. K. & SMITH, R. L. 1992. Ionic coupling among cells in the organ of Corti. *Hear Res,* 57**,** 175-94.

FIGURES

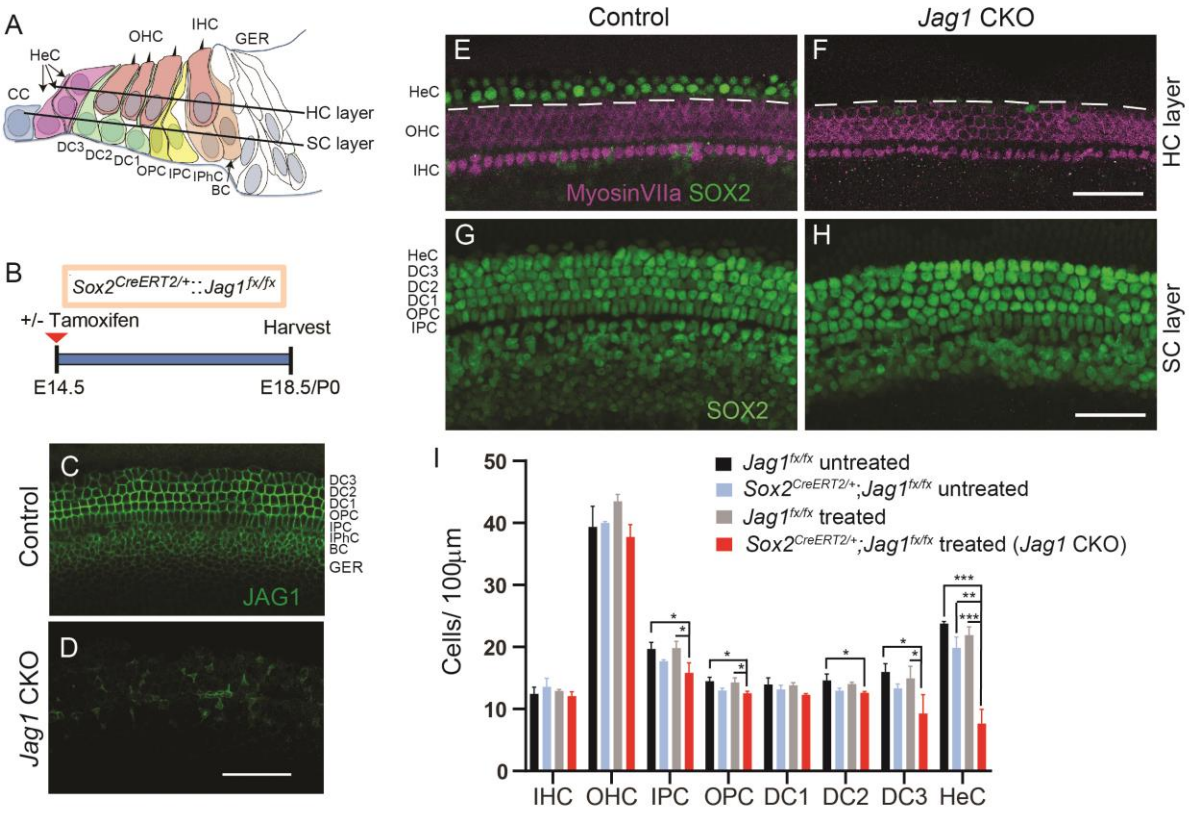

Figure 1. Deletion of *Jag1* from stage E14.5 progenitor cells disrupts HeC formation. (A) Schematic of the cellular composition of the neonatal auditory sensory epithelium. Abbreviations: BC, Border cell; CC, Claudius cell; DC1, Deiters' cell row 1; DC2, Deiters' cell row 2; DC3, Deiters' cell row 3; GER, greater epithelial ridge; HeC, Hensen's cell; HC, hair cell; IHC, inner hair cell; IPC, inner pillar cell; OHC, outer hair cell; OPC, outer pillar cell; SC, supporting cell. **(B)** Experimental strategy. Timed pregnant dams were injected with tamoxifen and progesterone at E14.5. *Jag1* conditional knockout (CKO) (*Sox2*$^{CreERT2/+}$*::Jag1*$^{fx/fx}$ treated) mice and control (*Jag1*$^{fx/fx}$ treated) littermates were analyzed at E18.5/P0. SOX2 immuno-staining labels SC nuclei including HeCs, while myosin VIIa immuno-staining labels IHCs and OHCs. Representative confocal images of

the cochlear mid-turn are shown. To control for *Sox2* haploinsufficiency, E18.5/P0 *Sox2*$^{CreERT2/+}$*::Jag1*$^{fx/fx}$ mice and *Jag1*$^{fx/fx}$ littermates that did not receive tamoxifen and progesterone (untreated) were also analyzed. **(C-D)** Validation of *Jag1* deletion. SC nuclear layer, immuno-stained for JAG1 (green), in *Jag1* CKO (D) and control (C, treated, *Jag1*$^{fx/fx}$) mice. **(E-F)** HC and HeC phenotype in P0 control (E, *Sox2*$^{CreERT2/+}$*::Jag1*$^{fx/fx}$ untreated*)* and P0 *Jag1* CKO (F) mice. Note control mice (E) contain 1-2 rows of SOX2^{+} (green) HeCs lateral to the myosin VIIa^{+} (magenta) OHCs (dashed white line) (see schematic in A). **(G-H)** SC phenotype in E18.5 control (G, *Jag1*$^{fx/fx}$ treated) and E18.5 *Jag1* CKO (H) mice. Note that DC nuclei are enlarged and misaligned in *Jag1* CKO mice. **(I)** Quantification of HC and SC subtypes in control and *Jag1* CKO mice. Data expressed as mean ± SD (n=3/group; two-way ANOVA, with Bonferroni correction was used to calculate p-values, *p<0.05, **p ≤0.001, ***p≤0.0001). Scale bar: 50 μm.

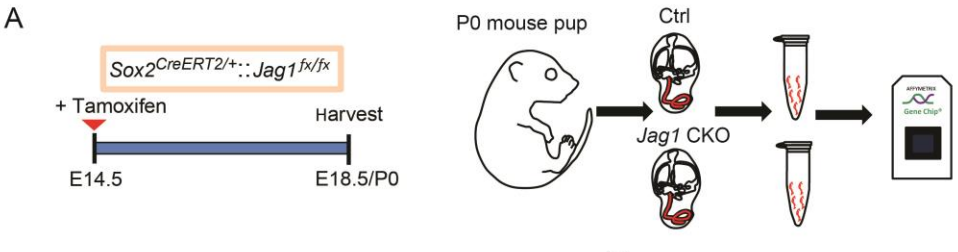

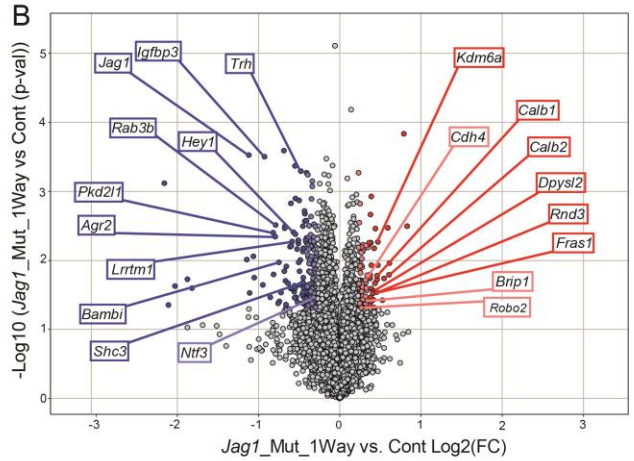

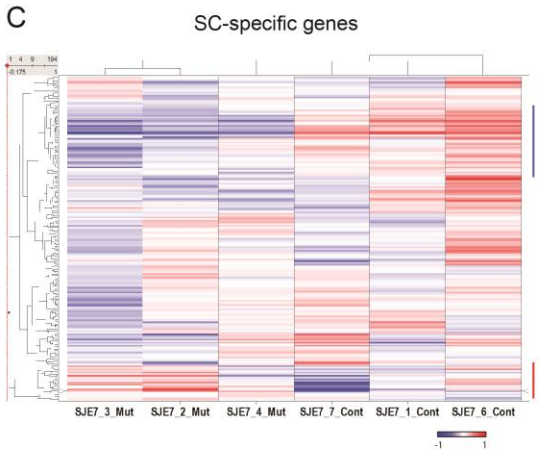

D

KEGG_PATHWAY	Count	%	P-value	Fold Enrich
mmu03010:Ribosome	16	3.8	1.0E-04	5.1
mmu05016:Huntington's disease	18	4.2	2.4E-04	4.2
mmu00190:Oxidative phosphorylation	15	3.5	3.4E-04	4.9
mmu05012:Parkinson's disease	15	3.5	7.8E-04	4.6
mmu05010:Alzheimer's disease	15	3.5	5.7E-03	3.9

E

GOTERM_CC_DIRECT	Count	%	P-value	Fold Enrich
GO:0005743~mitochondrial inner membrane	29	6.8	4.8E-07	4.0
GO:0070062~extracellular exosome	91	21.4	6.8E-06	1.8
GO:0005840~ribosome	16	3.8	1.0E-03	4.5
GO:0005739~mitochondrion	57	13.4	1.4E-02	1.7
GO:0022627~cytosolic small ribosomal subunit	8	1.9	1.9E-02	8.0
GO:0070469~respiratory chain	8	1.9	3.4E-02	7.3
GO:0030529~intracellular ribonucleoprotein complex	18	4.2	4.4E-02	3.0
GO:0005747~mitochondrial respiratory chain complex I	7	1.6	7.7E-02	7.9

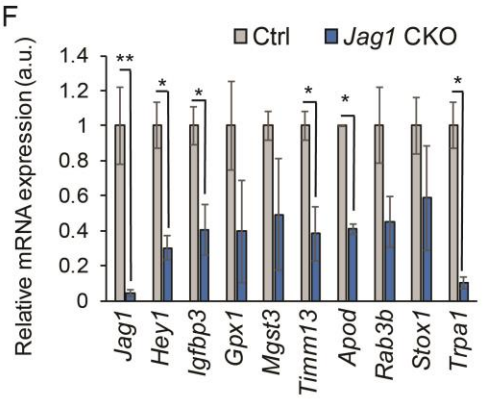

817

818 **Figure 2. Loss of JAG1 leads to the downregulation of genes involved in**
819 **mitochondrial function and protein synthesis. (A)** Experimental strategy. Timed
820 pregnant dams were injected with tamoxifen and progesterone at E14.5 and gene
821 expression in cochlear epithelia from E18.5/P0 *Jag1* conditional knockout (CKO),
822 (*Sox2*$^{CreERT2/+}$*::Jag1*$^{fx/fx}$) mice and control (Ctrl, *Jag1*$^{fx/fx}$) littermates was analyzed using
823 Clariom D mouse arrays. **(B)** Volcano plot presents the one-way ANOVA analysis of
824 differential gene expression in *Jag1* CKO versus control samples (n=3 animals/group).

Plotted as log2 fold-change (FC) (x-axis) versus −log10 p-value (y-axis). Dark blue (log2 (FC) <-6σ) and light blue (log2 (FC) <-3σ) dots represent downregulated genes. Dark red (log2 (FC) >6σ) and light red dots (log2 (FC) >3σ) represents upregulated genes. **(C)** Heat cluster map illustrating JAG1-mediated effects on a list of 200 SC-specific genes curated from published data. **(D-E)** Gene ontology (GO) analysis of genes down-regulated (p-value ≤0.05, log2 (FC) ≤2σ) in P0 *Jag1* CKO versus control (Ctrl) cochlear epithelia. Listed are significantly enriched (Bonferroni corrected p-value ≤0.05) pathways (D) and cellular component (E) GO terms. **(F)** RT-qPCR-based validation of genes of interest that were downregulated at P0 in *Jag1* CKO cochlear epithelia compared to Ctrl. Data expressed as mean ± SEM (minimum of n=3 animals/ group, two-tailed Students t-test was used to calculate p-values, *p<0.05, **p ≤0.001).

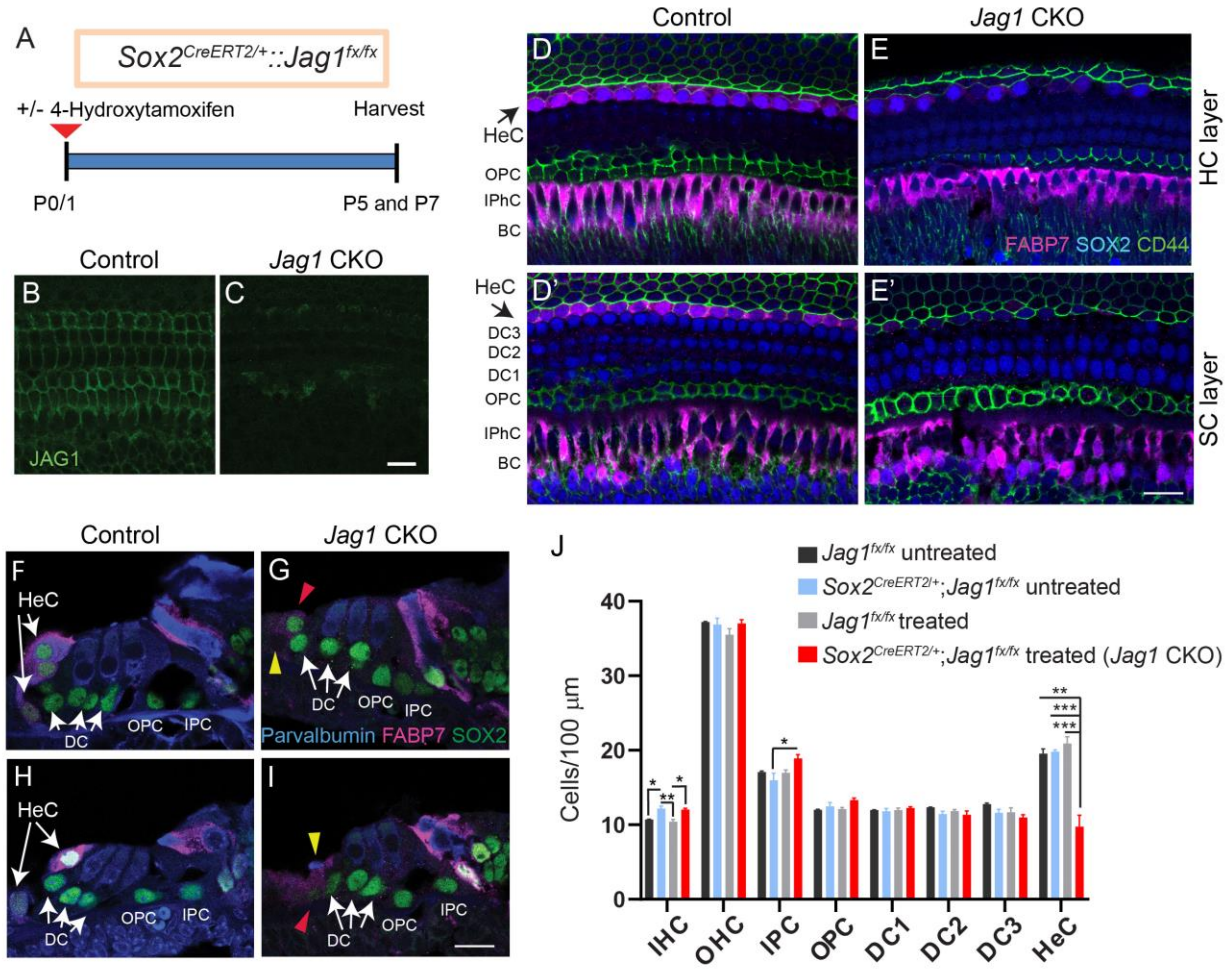

Figure 3. Deletion of *Jag1* from neonatal SCs results in the loss of HeCs. (A) Experimental strategy. *Sox2*$^{CreERT2/+}$*::Jag1*$^{fx/fx}$ and *Jag1*$^{fx/fx}$ were treated with 4-hydroxy-tamoxifen at P0/P1 and their cochleae were analyzed at P5 or P7. Untreated control mice (*Sox2*$^{CreERT2/+}$*::Jag1*$^{fx/fx}$ untreated and *Jag1*$^{fx/fx}$, untreated) were also used. SOX2 immuno-staining labels SC nuclei including HeCs. FABP7 labels HeCs, IPhCs and BCs. Parvalbumin labels HCs and CD44 labels CCs and OPCs. Shown are representative single plane confocal images of the cochlear mid-turn. **(B-C)** Validation of conditional *Jag1* deletion. Shown is the SC nuclear layer, immuno-stained for JAG1 (green), in *Jag1* CKO (C) and control (B, *Jag1*$^{fx/fx}$ treated) mice. **(D-E')** Top down view of the HC (D, E)

and SC nuclear layers (D', E') in *Jag1* CKO (E, E') and control (D, D', *Sox2*$^{CreERT2/+}$*::Jag1*$^{fx/fx}$ untreated) mice. Black arrows indicate the location of HeCs residing within the HC (D) and SC layer (D') in control mice. **(F-I)** Cochlear cross-sections of *Jag1* CKO (G, I) and control mice (F, H, *Sox2*$^{CreERT2/+}$*::Jag1*$^{fx/fx}$, untreated). White arrows indicate 2-3 HeC nuclei that are stacked on top of each other in control mice. Red arrowheads indicate SOX2^{+} HeC-like cells (G, I) and yellow arrowheads indicate dying cell (I) and missing HeC (G) in *Jag1* CKO mice. **(J)** Quantification of HC and SC subtypes in control and *Jag1* CKO mice. Data expressed as mean ± SD (n=3/ group; two-way ANOVA, with Bonferroni correction was used to calculate p-values, *p<0.05, **p ≤0.001, ***p≤0.0001). Abbreviations: IHC, inner hair cell; OHC, outer hair cell; IPC, inner pillar cell; OPC, outer pillar cell; DC1, Deiters' cell row 1; DC2, Deiters' cell row 2; DC3, Deiters' cell row 3; HeC, Hensen's cell. Scale bar: 20 μm.

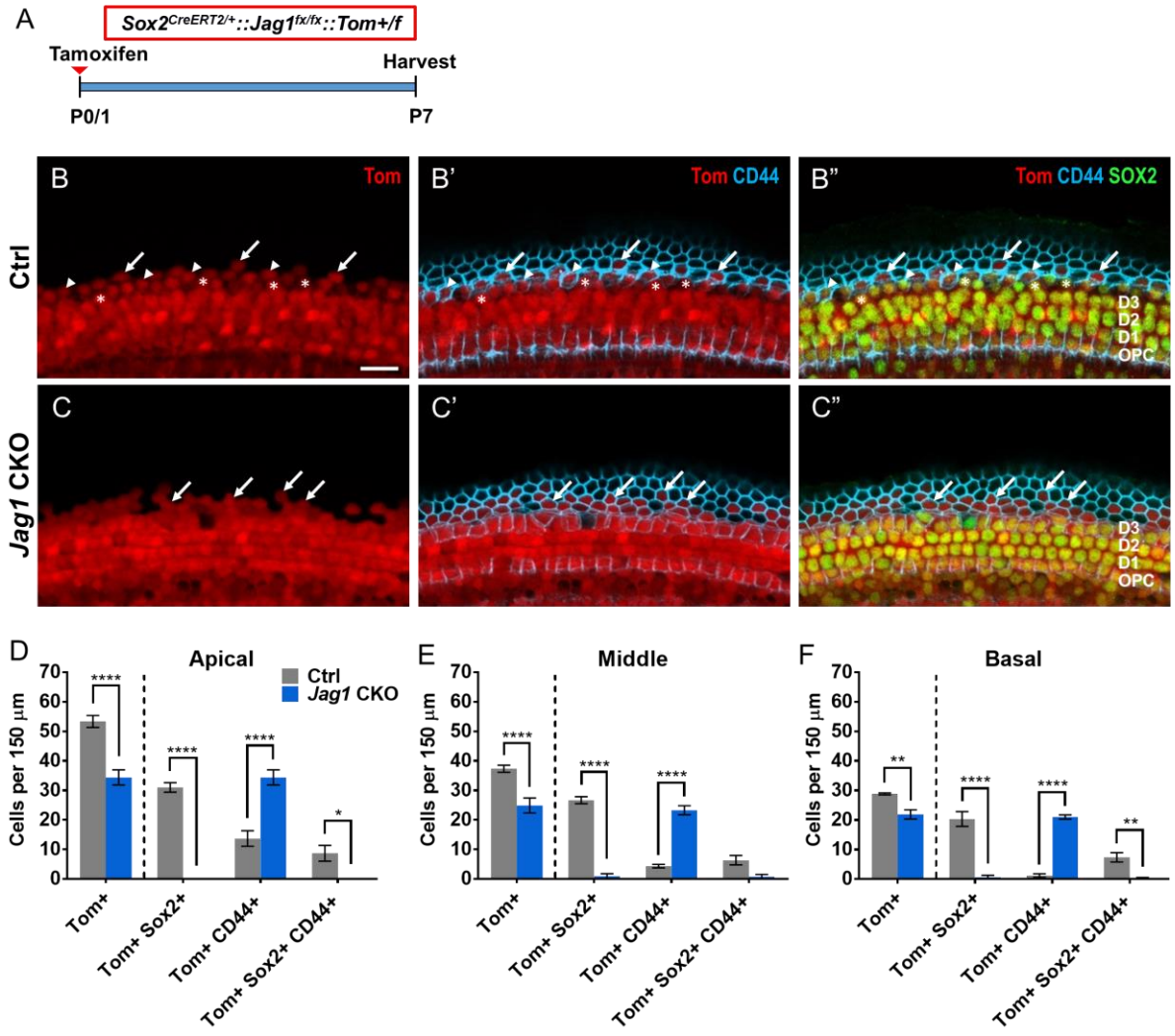

Figure 4. Fate-mapping analysis reveals that HeCs die or convert into CCs after deletion of *Jag1*. (A) Experimental strategy. *Sox2*$^{CreERT2/+}$*::Jag1*$^{fx/fx}$*::Rosa26*$^{tdTomato/+}$ (*Jag1* CKO) and *Sox2*$^{CreERT2/+}$*::Rosa26*$^{tdTomato/+}$ (Ctrl) mice were injected with tamoxifen at P0/P1 and cochleae were analyzed at P7. **(B-C")** Representative confocal images of the apical turn at P7 in Ctrl (B-B") and *Jag1* CKO (C-C") mice, showing expression of SOX2 (a SC marker, green), CD44 (a CC marker, blue) and tdTomato (Tom, red). Arrows indicate Tom$^+$, CD44$^+$ cells, * indicate Tom$^+$, SOX2$^+$ cells, and arrowheads indicate Tom$^+$, SOX2$^+$, CD44$^+$ cells. **(D-F)** Quantification of Tom$^+$ cells lateral to the 3rd row of DCs that

877 also express CD44 and/or SOX2 in the apical (D), middle (E), and basal (F) turns of the
878 cochleae in Ctrl and *Jag1* CKO mice. Data are expressed as mean ± SEM. n=3-4/group;
879 *p<0.05, **p<0.01, ****p<0.0001. Scale bar: 20 μm.

880

881

882

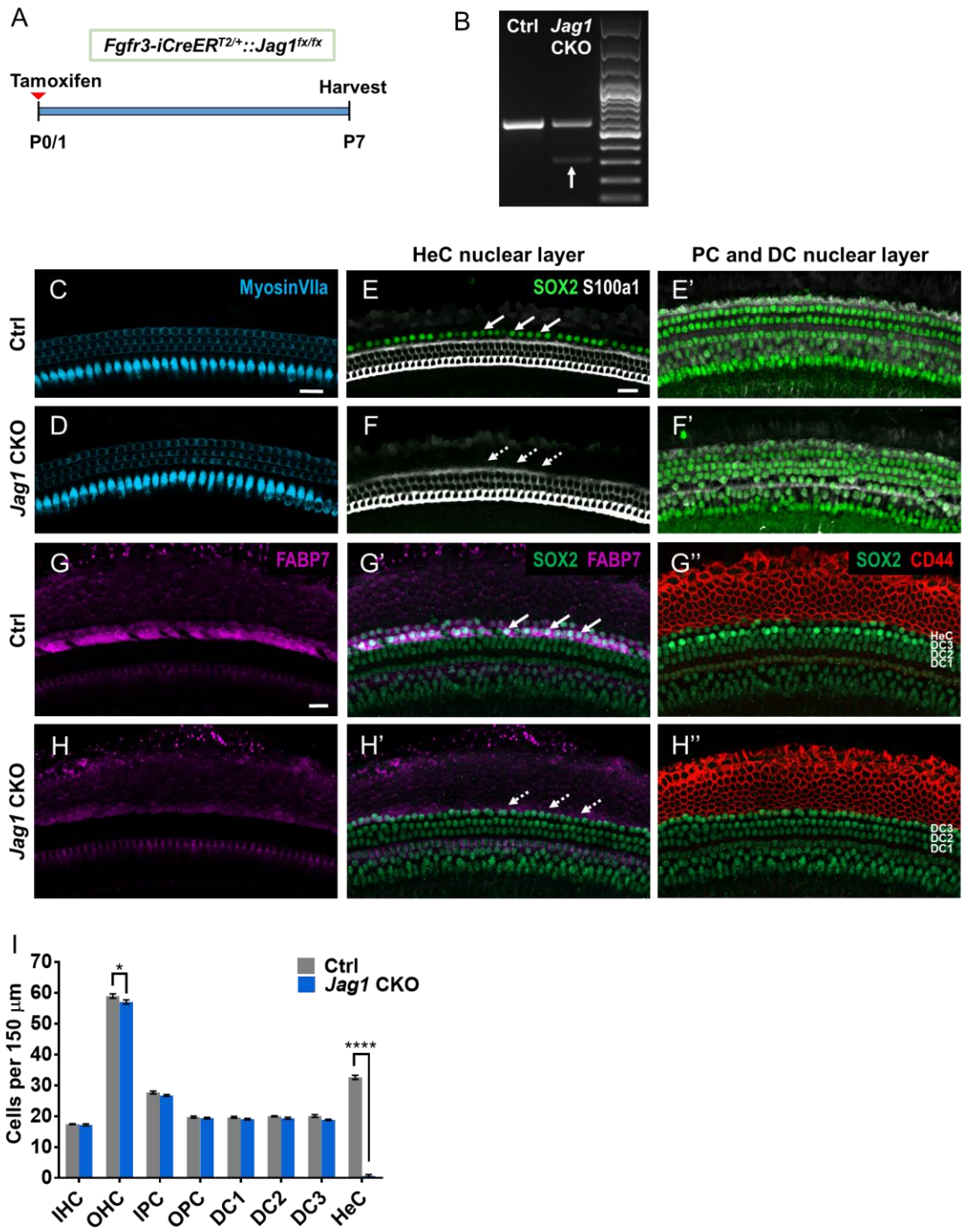

Figure 5. Massive loss of HeCs at P7 after neonatal deletion of *Jag1* from PCs and DCs. (A) Experimental strategy. *Fgfr3-iCreER*$^{T2/+}$::*Jag1*$^{fx/fx}$ (*Jag1* CKO) and *Jag1*$^{fx/fx}$ (Ctrl) mice were injected with tamoxifen at P0/P1 and cochleae were analyzed at P7. **(B)** RT-

887 PCR results using RNA extracted from P7 Ctrl and *Jag1* CKO whole cochlea. The upper
888 band (541 bp) indicates the wild-type allele containing exon 4. The lower band (286 bp,
889 white arrow) confirms deletion of *Jag1* exon 4 in *Jag1* CKO mice. The upper band is still
890 present in *Jag1* CKO mice since JAG1 Is expressed in all SCs and *Fgfr3-iCreER*$^{T2/+}$ only
891 targets PCs and DCs. **(C-D)** Representative confocal slice images of HC, labeled with
892 myosin VIIa (blue) in P7 Ctrl (C) and *Jag1* CKO (D) mice. **(E-F')** Representative confocal
893 slice images of SC nuclear layers at the level of HeC nuclei (E, F) and at the level of
894 PC/DC nuclei (E', F') showing SOX2 (a SC marker, green) and S100a1 (a PC and DC
895 marker, white) expression in P7 Ctrl (E-E') and *Jag1* CKO (F-F') mice. Arrows indicate
896 the location of HeCs (E, F). **(G-H")** Representative confocal slice images of SOX2
897 (green), FABP7 (a HeC marker, magenta), and CD44 (a CC marker, red) expression in
898 P7 Ctrl (G-G") and *Jag1* CKO (H-H") mice. Arrows indicate the location of HeCs (G', H').
899 **(I)** Quantification of IHCs, OHCs, and individual SC subtypes (IPCs to HeCs) in Ctrl and
900 *Jag1* CKO mice. Data are expressed as mean ± SEM. n=4/group; *p<0.05, ****p<0.0001.
901 Abbreviations: IHC, inner hair cell; OHC, outer hair cell; IPC, inner pillar cell; OPC, outer
902 pillar cell; DC1, Deiters' cell row 1; DC2, Deiters' cell row 2; DC3, Deiters' cell row 3; HeC,
903 Hensen's cell. Scale bar: 20 μm.
904
905
906

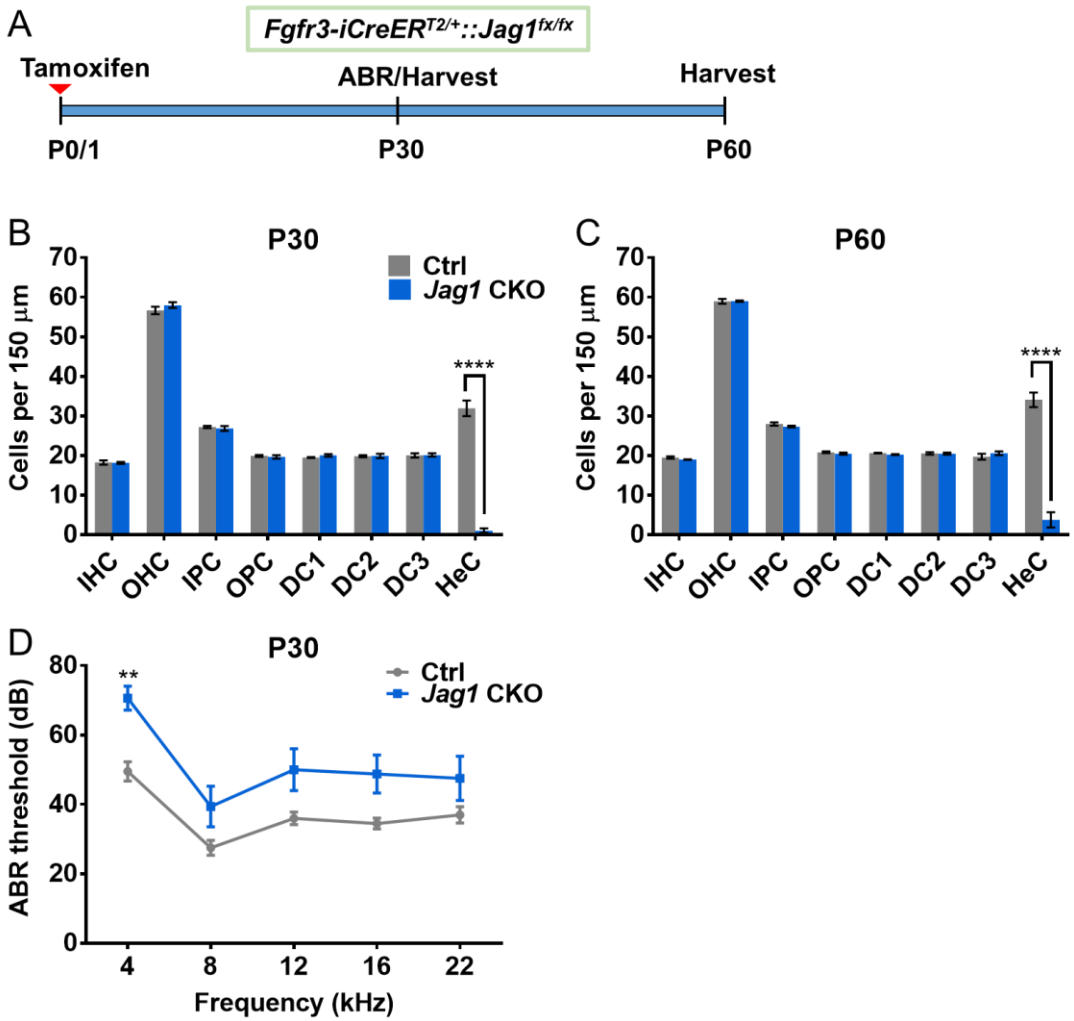

Figure 6. Neonatal *Jag1* deletion from PCs and DCs caused hearing deficits in the low frequency range. (A) Experimental strategy. *Fgfr3-iCreER*$^{T2/+}$*::Jag1*$^{fx/fx}$ (*Jag1* CKO) and *Jag1*$^{fx/fx}$ (Ctrl) mice were injected with tamoxifen at P0/P1, followed by ABR at P30, and analysis of the cochlea at P30 or P60. **(B-C)** Quantification of IHCs, OHCs, and individual SC subtypes (IPCs to HeCs) in Ctrl and *Jag1* CKO mice at P30 (B) and P60 (C). Data are expressed as mean ± SEM. n=4/group; ****p<0.0001. **(D)** ABR thresholds of Ctrl and *Jag1* CKO at P30. Data are expressed as mean ± SEM. n=8-10/group; **p<0.01. Abbreviations: IHC, inner hair cell; OHC, outer hair cell; IPC, inner pillar cell;

916 OPC, outer pillar cell; DC1, Deiters' cell row 1; DC2, Deiters' cell row 2; DC3, Deiters' cell

917 row 3; HeC, Hensen's cell.

918

919

920

921

922

923

924

925

926

927

928

929

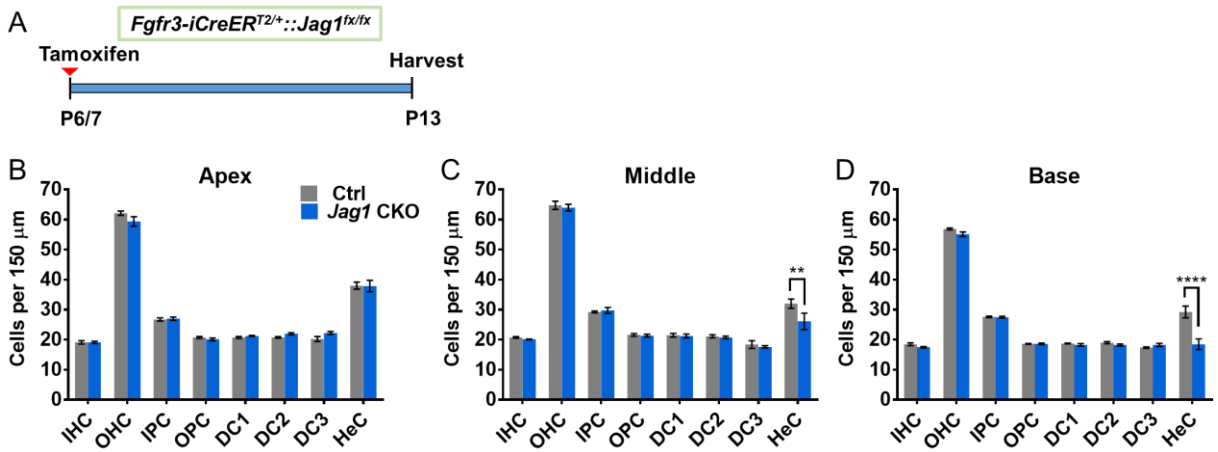

Figure 7. Mild loss of HeCs after deletion of *Jag1* from PCs and DCs at one week of age. (A) Experimental strategy. *Fgfr3-iCreER*$^{T2/+}$*::Jag1*$^{fx/fx}$ (*Jag1* CKO) and *Jag1*$^{fx/fx}$ (Ctrl) mice were injected with tamoxifen at P6/P7 and cochleae are analyzed at P13. **(B-D)** Quantification of IHCs, OHCs, and individual SC subtypes (IPCs to HeCs) in the apical (B), middle (C), and basal (D) turns of the cochleae in Ctrl and *Jag1* CKO mice at P13. Data are expressed as mean ± SEM. n=4/group; **p<0.01, ****p<0.0001. Abbreviations: IHC, inner hair cell; OHC, outer hair cell; IPC, inner pillar cell; OPC, outer pillar cell; DC1, Deiters' cell row 1; DC2, Deiters' cell row 2; DC3, Deiters' cell row 3; HeC, Hensen's cell.

SUPPLEMENTAL MATERIAL

Supplemental Table 1. List of top-ranked down-regulated genes after *Jag1* deletion. Genes are ranked based on fold change. Shown are genes that are significantly down-regulated in *Jag1* CKO samples compared to control (p-value ≤0.05, log2 (FC) ≤3σ) after tamoxifen and progesterone injection at E14.5. $ marks SC-specific/enriched genes (Maass et al., 2016, Burns et al., 2015) and # marks genes previously found to be positively regulated in cochlear epithelial cells by Notch signaling (Maass et al., 2016, Campbell et al., 2016). Note that only transcripts with mean log2 values of 5.5 or more in control samples are listed.

Gene Symbol	Accession ID	P-Value	Mean log2 Ctrl	Mean log2 Jag1 mut	Fold Change
Npy[$]	NM_023456	0.0008	9.68	7.52	-4.47
Hbb-bt	NM_008220	0.0443	9.82	7.71	-4.31
Emcn	NM_001163522	0.0190	6.85	4.97	-3.67
Hba-a2	NM_001083955	0.0254	9.60	7.78	-3.53
Prss3	NM_011645	0.0098	6.89	5.74	-2.21
Jag1[$,#]	NM_013822	0.0003	10.75	9.64	-2.17
Hbb-bs	NM_001201391	0.0297	8.13	7.02	-2.16
Car14[$]	NM_011797	0.0088	7.23	6.17	-2.09
Foxf2	NM_010225	0.0179	6.29	5.24	-2.07
Bgn	NM_007542	0.0229	7.51	6.57	-1.92
Igfbp3[$,#]	NM_008343	0.0003	9.20	8.27	-1.90
Ccn3	NM_010930	0.0347	6.51	5.65	-1.81
Pkd2l1[$]	NM_181422	0.0040	6.46	5.64	-1.77
Gm10334	NM_001103153	0.0161	7.10	6.28	-1.76
Agr2	NM_011783	0.0046	7.47	6.67	-1.73
Rab3b[$,#]	NM_023537	0.0031	7.91	7.13	-1.73
Ifitm3	NM_025378	0.0421	6.85	6.09	-1.69
Bambi	NM_026505	0.0107	8.14	7.40	-1.68
Rgs2	NM_009061	0.0145	7.15	6.46	-1.61
Fkbp11	NM_024169	0.0032	7.99	7.32	-1.59
Emilin2[$]	NM_145158	0.0199	6.87	6.20	-1.59
St3gal1	NM_009177	0.0064	7.90	7.29	-1.53

Agr3[$,#]	NM_207531	0.0259	7.65	7.05	-1.51
Aldh1a7	NM_011921	0.0015	6.30	5.71	-1.51
Ccn4	NM_018865	0.0062	7.72	7.13	-1.51
Lrrtm1[$,#]	NM_028880	0.0053	7.37	6.79	-1.50
Tyrobp	NM_011662	0.0261	6.60	6.03	-1.48
Pthlh	NM_008970	0.0039	7.84	7.27	-1.48
S100a6[$]	NM_011313	0.0255	6.38	5.83	-1.46
A830018L16Rik	NM_001160369	0.0004	6.23	5.68	-1.46
Stox1[$]	NM_001033260	0.0013	8.50	7.95	-1.46
Hey1[$,#]	NM_010423	0.0042	11.50	10.96	-1.46
AU021092	NM_001033220	0.0344	6.98	6.45	-1.45
Gm5771	NM_001038997	0.0069	6.37	5.85	-1.44
Cavin3[$]	NM_028444	0.0052	9.73	9.22	-1.42
Trh[$,#]	NM_009426	0.0005	6.10	5.62	-1.39
Cntfr	NM_001136056	0.0313	8.33	7.87	-1.38
Pifo	NM_001200028	0.0414	6.81	6.36	-1.37
Shc3[$,#]	NM_009167	0.0209	8.18	7.73	-1.37
Plagl1	NM_009538	0.0075	6.73	6.28	-1.37
Antxr1	NM_054041	0.0068	9.29	8.84	-1.37
Jam2	NM_023844	0.0179	5.95	5.50	-1.36
Borcs8	NM_001145552	0.0320	8.11	7.66	-1.36
Foxq1	NM_008239	0.0251	7.53	7.09	-1.44
Timm13[$]	NM_013895	0.0221	9.84	9.40	-1.35
Cnrip1	NM_029861	0.0435	6.52	6.08	-1.35
Mansc4[$]	NM_001034903	0.0027	6.03	5.60	-1.34
Prss1	NM_053243	0.0021	6.57	6.15	-1.34
Mir5103	NR_039562	0.0051	6.87	6.45	-1.33
Hebp1	NM_013546	0.0286	7.44	7.03	-1.33
Snord123	NR_028575	0.0054	7.96	7.55	-1.33
Pipox	NM_008952	0.0005	6.59	6.18	-1.32
Vkorc1	NM_178600	0.0297	11.41	11.00	-1.32
Ddt	NM_010027	0.0048	7.40	6.99	-1.32
Polr2i	NM_027259	0.0464	8.55	8.15	-1.31
Mgst3[$]	NM_025569	0.0497	10.13	9.74	-1.35
Lsamp[$,#]	NM_175548	0.0059	7.60	7.21	-1.35
Nkain4	NM_001141933	0.0006	7.35	6.95	-1.31
Lgals9	NM_001159301	0.0083	7.05	6.66	-1.31
Mir193b	NR_030549	0.0357	6.68	6.30	-1.31
Gstm5	NM_010360	0.0475	10.04	9.66	-1.31
Kcnj4	NM_008427	0.0433	5.78	5.40	-1.30
Ank	NM_020332	0.0405	9.81	9.43	-1.30

Gm10941	NR_026944	0.0040	7.31	6.93	-1.30
Car10[$]	NM_028296	0.0070	6.30	5.92	-1.30
Fbn1[#]	NM_007993	0.0111	6.86	6.48	-1.30
Ndufb4b	XM_001478443.2	0.0145	10.53	10.15	-1.30
Snhg18	NR_038186	0.0032	7.92	7.55	-1.30
Mfge8	NM_001045489	0.0227	7.65	7.27	-1.30
Gpx1[$,#]	NM_008160	0.0231	10.46	10.09	-1.30
Fbln1	NM_010180	0.0455	7.05	6.68	-1.29
Cmtm3	NM_024217	0.0247	8.57	8.20	-1.29
E030030I06Rik[$]	NM_001254744	0.0441	6.70	6.33	-1.29
Kit	NM_001122733	0.0099	7.62	7.26	-1.29
Dpysl4[$]	NM_011993	0.0251	8.76	8.40	-1.29
Lrrc51	NM_001162973	0.0277	8.16	7.80	-1.29
1810044D09Rik	NR_038153	0.0146	5.80	5.44	-1.29
Pold4	NM_027196	0.0247	8.53	8.17	-1.28
Bst2	NM_198095	0.0227	7.02	6.66	-1.28
B3gnt7	NM_145222	0.0379	7.85	7.49	-1.28
Insl6	NM_013754	0.0063	8.16	7.80	-1.28
Timp1	NM_001044384	0.0154	6.34	5.99	-1.28
Sft2d3	NM_026006	0.0023	7.72	7.36	-1.27
Fscn1	NM_007984	0.0344	7.74	7.39	-1.27
Gsto1[$]	NM_010362	0.0013	6.07	5.72	-1.27
BC035947	BC138135	0.0087	6.73	6.39	-1.27
Etv1[$,#]	NM_001163154	0.0114	6.98	6.63	-1.27
A330009N23Rik	NR_045326	0.0482	6.69	6.35	-1.27
Rufy4[$]	NM_001034060	0.0424	7.12	6.78	-1.27
Mdm1[$]	NM_001162904	0.0105	7.85	7.51	-1.26
Nme9	NM_001165957	0.0007	6.05	5.71	-1.26
Fli1	NM_008026	0.0275	6.07	5.74	-1.26
Mtln	NR_015476	0.0261	8.31	7.97	-1.26
Rras[$,#]	NM_009101	0.0009	9.48	9.15	-1.26
Psmg4	NM_001101430	0.0050	9.29	8.96	-1.26
Setmar	NM_001276356	0.0270	6.73	6.41	-1.25
F2rl1[$,#]	NM_007974	0.0193	7.49	7.17	-1.25
Cenpn	NM_028131	0.0460	6.19	5.87	-1.25
Nenf	NM_025424	0.0449	8.88	8.56	-1.25
Ntf3[$,#]	NM_001164034	0.0345	7.67	7.35	-1.25
Glul	NM_008131	0.0053	8.32	8.00	-1.25
Reps2	NM_178256	0.0152	7.03	6.72	-1.25
Adat2	NM_025748	0.0030	8.61	8.29	-1.25
Lrfn2	NM_027452	0.0493	6.20	5.89	-1.25

Ill10ra	NM_008348	0.0090	5.74	5.42	-1.24
Mir7020	NR_105987	0.0047	6.32	6.00	-1.24
Sept4	NM_001284392	0.0070	6.50	6.18	-1.24
Commd4	NM_025417	0.0225	9.80	9.49	-1.24
Lsm4	NM_015816	0.0394	9.79	9.47	-1.24
Selenoh	NM_001033166	0.0302	8.75	8.43	-1.24
Cxcl12[#]	NM_001012477	0.0340	6.31	6.00	-1.24
Slc2a3	NM_011401	0.0071	5.81	5.50	-1.24
Atp5g1	NM_001161419	0.0215	8.58	8.27	-1.24
Zmat5	NM_026015	0.0485	8.33	8.02	-1.24
Adgre5	NM_001163029	0.0367	6.45	6.14	-1.25
Sp7	NM_130458	0.0490	5.97	5.66	-1.24
1700003D09Rik	NR_045477	0.0252	6.06	5.75	-1.24
Wdr83os	NM_001001493	0.0246	9.24	8.94	-1.24
Mettl26	NM_026686	0.0439	9.53	9.23	-1.23
Nit2	NM_023175	0.0485	7.68	7.38	-1.23
Ndufa3	NM_025348	0.0345	9.34	9.03	-1.23
Ppih	NM_001110129	0.0033	7.78	7.48	-1.23
Rps15	NM_009091	0.0424	11.11	10.81	-1.23
5730408K05Rik	NR_027866	0.0183	6.54	6.25	-1.23
Ndufaf3	NM_023247	0.0105	7.31	7.01	-1.23
Scarna6	NR_028519	0.0483	6.31	6.02	-1.23
Gm9258	XR_105855.1	0.0305	7.00	6.70	-1.23
Ppp1r1a	NM_021391	0.0225	7.95	7.65	-1.23
Lsm7	NM_025349	0.0324	8.80	8.51	-1.22
Dpm2	NM_010073	0.0099	7.75	7.46	-1.22
Rtl8c	NM_028375	0.0065	7.17	6.88	-1.22
Ciao2b	NM_026753	0.0408	8.96	8.67	-1.22
Muc1[$,#]	NM_013605	0.0078	6.94	6.65	-1.22
Smim3[$]	NM_134133	0.0270	7.30	7.01	-1.22
Nop10	NM_025403	0.0196	7.30	7.02	-1.22
Mrpl36[$]	NM_053163	0.0171	7.69	7.41	-1.22
Ndufb4	NM_026610	0.0260	7.66	7.37	-1.22
Nkapl	NM_025719	0.0179	6.06	5.78	-1.21
Pard6g	NM_053117	0.0383	7.79	7.51	-1.21
Rps26	NM_013765	0.0416	12.42	12.15	-1.21

954

955

Supplemental Table 2. List of top-ranked up-regulated genes after *Jag1* deletion. Genes are ranked based on fold change (FC). Shown are genes that are significantly up-regulated in *Jag1* CKO samples compared to control (p-value ≤0.05, log2 (FC) ≥3σ) after tamoxifen and progesterone injection at E14.5. $ marks SC-specific/enriched genes (Maass et al., 2016, Burns et al., 2015) and # marks genes previously found to be negatively regulated in cochlear epithelial cells by Notch signaling (Maass et al., 2016, Campbell et al., 2016). Note that only transcripts with mean log2 values in Jag1 mutant samples of 5.5 or more are listed.

Gene Symbol	Accession ID	P-Value	Mean Log2 Ctrl	Mean Log2 Jag1 mut	Fold Change
Brinp1	NM_019967	0.0032	7.14	7.97	1.78
Tmem132d	NM_172885	0.0111	7.67	8.28	1.53
Calb2	NM_007586	0.0164	7.09	7.70	1.53
Crhbp	NM_198408	0.0034	5.55	6.14	1.51
Kcne1	NM_008424	0.0183	5.32	5.87	1.46
Tmem117	NM_178789	0.0377	8.44	8.97	1.44
Plxna4	NM_175750	0.0529	8.643	9.12	1.40
Kdm6a	NM_009483	0.0054	7.96	8.44	1.39
Calb1	NM_009788	0.0168	9.43	9.89	1.38
Rnd3[$]	NM_028810	0.0291	7.80	8.26	1.37
Cdkl1	NM_183294	0.0035	5.25	5.70	1.36
Eif2s3x	NM_012010	0.0215	8.03	8.47	1.35
Asic3	NM_183000	0.0489	8.91	9.34	1.35
Dennd4a	NM_001162917	0.0525	8.27	8.69	1.34
Vmn1r90	NM_001244031	0.0295	5.57	6.00	1.34
Dpysl2[$,#]	NM_009955	0.0277	10.75	11.17	1.34
B4galnt3[$]	NM_198884	0.0372	9.88	10.30	1.34
Fras1	NM_175473	0.0303	9.89	10.30	1.33
Meltf	NM_013900	0.0369	8.54	8.94	1.32
Fam184b	NM_021416	0.0257	8.34	8.73	1.31
Olfr1383	NM_207574	0.0012	5.62	6.01	1.31
Phactr1	NM_001005740	0.0401	6.12	6.50	1.31
Iigp1	NM_001146275	0.0056	6.06	6.44	1.31
Ano1[$]	NM_001242349	0.0403	8.66	9.04	1.30

Elovl7	NM_029001	0.0059	5.62	5.99	1.29
Twf1	NM_008971	0.0066	10.13	10.48	1.28
Brip1[$]	NM_178309	0.0384	5.98	6.32	1.27
Kdsr[$]	NM_027534	0.0486	9.59	9.93	1.26
Tex19.2	NM_027622	0.0274	5.41	5.75	1.26
Cpa6[$,#]	NM_001289497	0.0255	6.86	7.18	1.26
Daam1	NM_001286452	0.0211	8.42	8.75	1.25
Vps4b	NM_009190	0.0426	8.43	8.75	1.25
Ctrcos	NR_040641	0.0062	6.69	7.01	1.25
Ptgir[$]	NM_008967	0.0437	6.01	6.33	1.25
Cdh4[#]	NM_009867	0.0195	10.22	10.55	1.25
Atp1b1	NM_009721	0.0334	10.58	10.90	1.25
Kdm5c	NM_013668	0.0251	8.44	8.75	1.24
Tnnc2	NM_009394	0.0510	6.84	7.14	1.23
Cdh11	NM_009866	0.0329	10.58	10.87	1.22
Fut2	NM_001271993	0.0535	6.23	6.52	1.22
Dpyd	NM_170778	0.0480	7.86	8.15	1.22
Mertk	NM_008587	0.0368	8.06	8.34	1.22
Kcnq5	NM_001160139	0.0242	5.98	6.26	1.22
Rxrg	NM_001159731	0.0480	8.23	8.50	1.21
Pou3f2	NM_008899	0.0078	5.38	5.65	1.21
Robo2[#]	NM_175549	0.0487	8.71	8.98	1.21
Peg3	NM_008817	0.0065	8.65	8.91	1.20
Epyc	NM_007884	0.0194	12.88	13.14	1.20
Corin[$]	NM_001122756	0.0286	6.31	6.57	1.20
Ppp2r3a	NM_001161362	0.0153	6.55	6.81	1.20
Tmem266	NM_172923	0.0345	6.78	7.04	1.19
Sft2d2	NM_145512	0.0122	7.45	7.70	1.19
Mir181c	NR_029821	0.0198	7.77	8.02	1.19
Adamts17	NM_001033877	0.0256	9.11	9.36	1.19
Serpinb5	NM_009257	0.0422	7.02	7.27	1.19

964

965

966

967